Mitochondrial Function and Maize Kernel Development Requires Dek2, a Pentatricopeptide Repeat Protein Involved in nad1 mRNA Splicing

Weiwei Qi,*,[1] Yang Yang,*,[1] Xuzhen Feng,* Mingliang Zhang,[†] and Rentao Song*,[†,2]
*Shanghai Key Laboratory of Bio-Energy Crops, School of Life Sciences, Shanghai University, Shanghai 200444, China and
[†]National Maize Improvement Center of China, China Agricultural University, Beijing 100193, China

ABSTRACT In flowering plants, many respiration-related proteins are encoded by the mitochondrial genome and the splicing of mitochondrion-encoded messenger RNA (mRNA) involves a complex collaboration with nuclear-encoded proteins. Pentatricopeptide repeat (PPR) proteins have been implicated in these RNA–protein interactions. Maize *defective kernel 2* (*dek2*) is a classic mutant with small kernels and delayed development. Through positional cloning and allelic confirmation, we found *Dek2* encodes a novel P-type PPR protein that targets mitochondria. Mitochondrial transcript analysis indicated that *dek2* mutation causes reduced splicing efficiency of mitochondrial *nad1* intron 1. Mitochondrial complex analysis in *dek2* immature kernels showed severe deficiency of complex I assembly. Dramatically up-regulated expression of *alternative oxidases* (*AOXs*), transcriptome data, and TEM analysis results revealed that proper splicing of *nad1* is critical for mitochondrial functions and inner cristaes morphology. This study indicated that *Dek2* is a new PPR protein that affects the splicing of mitochondrial *nad1* intron 1 and is required for mitochondrial function and kernel development.

KEYWORDS *Zea mays*; *dek2*; pentatricopeptide repeat protein; mitochondrion; RNA splicing

MITOCHONDRIAL respiration is the core for cell free energy releasing and ATP production (Siedow and Day 2000). The electron transport chain (ETC) is composed of five respiratory complexes in mitochondrion (Dudkina *et al.* 2006). The mitochondrial genome possesses genes encoding proteins involved in ETC. The mitochondrial genome-expressed pre-RNAs can be post-transcriptionally processed, including RNA editing, RNA *cis*- and *trans*-splicing, RNA cleavage, and RNA maturation processes (Knoop 2013; Hammani and Giege 2014). Nuclear genome expressed pentatricopeptide repeat (PPR) proteins are reported to play a critical role in these processes (Barkan and Small 2014). The PPR proteins are defined by the tandem repeats of a degenerate 35-amino-acid motif and are classified into two major subgroups: the P-type PPR members only possess tandem repeats of the 35-amino-acid PPR motif, and the PLS-type PPR members composed of sequential repeats of P, short (S), and long (L) PPR motifs and often carry an E or E–DYW domain extension in the C terminus (Lurin *et al.* 2004; Cheng *et al.* 2016). The PPR family comprises >450 members in plants, and a number of severe growth and development defects associated with loss-of-function PPR mutants were described before (Fujii and Small 2011; Sosso *et al.* 2012; Liu *et al.* 2013; Colas des Francs-Small and Small 2014; Hammani and Giege 2014; Li *et al.* 2014; Sun *et al.* 2015; Chen *et al.* 2016; Haili *et al.* 2016; Xiu *et al.* 2016). However, the regulatory functions are still unknown for great numbers of unidentified PPR proteins.

P-type PPR proteins are dedicated to RNA stabilization, cleavage, translational activation, and splicing (Barkan and Small 2014; Xiu *et al.* 2016). Groups I and II introns are two kinds of introns with distinct splicing patterns. Group II introns are found in ribosomal (rRNA), transfer RNA (tRNA), bacterial messenger RNA (mRNA) and mRNA of organelles in fungi, plants, and protests. They are self-splicing ribozymes (Eickbush 1999). In plants, >20 group II introns exist in the mitochondrial genome, and most of them belong to genes

doi: 10.1534/genetics.116.196105
Manuscript received September 20, 2016; accepted for publication October 25, 2016; published Early Online November 4, 2016.
Supplemental material is available online at www.genetics.org/lookup/suppl/doi:10.1534/genetics.116.196105/-/DC1.
[1]These authors contributed equally to this work.
[2]Corresponding author: Shanghai Key Laboratory of Bio-Energy Crops, School of Life Sciences, Shanghai University, 333 Nanchen Rd., Shanghai 200444, China. E-mail: rentaosong@cau.edu.cn

encoding subunits in complex I, including 15 *cis*-spliced introns in *nad1*, *nad2*, *nad4*, *nad5*, *nad7*, *rps3*, *cox2*, *ccmFC* and 7 *trans*-spliced introns in *nad1*, *nad2*, and *nad5* (Burger *et al.* 2003; Berrisford and Sazanov 2009). Five P-type PPR proteins are reported to be necessary for group II intron splicing of mitochondrial transcripts in *Arabidopsis*, functioning in *nad1* (de Longevialle *et al.* 2007), *nad2* (Liu *et al.* 2010), *nad5* (Colas des Francs-Small *et al.* 2014), and *nad7* (Hsieh *et al.* 2015). In maize, EMP16 was reported to be involved in *nad2* intron 4 *cis*-splicing (Xiu *et al.* 2016), and DEK35 is required for *nad4* intron 1 *cis*-splicing (Chen *et al.* 2016). The important roles of more P-type PPR proteins in mitochondrial RNA *cis*- and *trans*-splicing processes can be revealed through studies on maize kernel mutants.

Maize (*Zea mays*) is suitable material for genetics research, partly because of its numerous easily observable phenotypes (Neuffer and Sheridan 1980). Defective kernel (dek) mutants are a major class of maize kernel mutants that are a good resource for investigating kernel development (Neuffer and Sheridan 1980). To date, many maize dek mutants have been identified: *dek1* causes severe growth and development defects (Lid *et al.* 2002); *reas1(dek*)* causes only mild developmental delay (Qi *et al.* 2016); and the mutants of PPRs, including *ppr2263*, *smk1*, *emp5*, *emp7*, *emp16*, and *dek35*, always have an obvious small kernel phenotype, with arrested development of embryo and endosperm (Liu *et al.* 2013; Li *et al.* 2014; Sun *et al.* 2015; Chen *et al.* 2016). Dek mutants offer opportunities to investigate many basic biological processes during kernel development.

In this study, we characterized maize classic mutant *dek2*, a defective kernel mutant with small kernels and delayed development. We report the map-based cloning of *Dek2* and demonstrate it encodes a P-type PPR in maize. We present evidence that Dek2 is specifically involved in the splicing of *nad1* intron 1. Lack of these splicing processes affects complex I accumulation. Consequently, it arrests mitochondrial oxidative phosphorylation and kernel development.

Materials and Methods

Plant materials

The maize *dek2-N1315A* stock was obtained from the Maize Genetics Cooperation Stock Center (http://www.maizegdb.org/data_center/stock?id=13997) as an EMS-induced mutant first described by Neuffer and Sheridan (1980). The mutant was crossed into a W22 genetic background to produce the F_2 populations. Kernels of the F_2 ears exhibited a 3:1 segregation of wild-type (WT) kernels (*dek2*/+ or +/+) and homozygous mutant kernels (*dek2*/*dek2*) were used for analysis. All the plants were cultivated in the field on the Shanghai University campus.

Measurement of protein and starch

For the protein measurements, the endosperm of *dek2* and WT mature kernels was separated from the embryo and pericarp by dissection after soaking the kernels in water. The samples were dried to constant weights, pulverized with a mortar and pestle in liquid N_2, and then measured according to a previously described protocol (Wang *et al.* 2011). All the measurements were replicated at least three times.

For the starch measurements, five mature kernels of the WT and *dek2* were ground in liquid N_2. The resulting powders were dried to a constant weight. Finally, the total starch was measured by using an amyloglucosidase/α-amylase starch assay kit (Megazyme). The protocol referenced the method by Wang *et al.* (2014). All the measurements were replicated at least three times.

Light microscopy

Immature WT and *dek2* kernels at 12 days after pollination (DAP) and 18 DAP were collected from F_2 ears and were cut along the longitudinal axis for paraffin and resin section preparation. The sections were fixed in formalin–acetic acid–alcohol mixture and were dehydrated in an ethanol gradient series of 50, 60, 70, 85, 95, and 100% ethanol. After replacement of acetone and infiltration with paraffin or resin, the sections were embedded and cut using Leica RM2265. The paraffin section was stained by fuchsin basic, and the resin section was stained by fuchsin basic (horizontal cut) and toluidine blue (longitudinal cut). The sections were observed using Leica DFC500.

Scanning electron microscopy and transmission electron microscopy

For scanning electron microscopy, *dek2* and WT kernels were prepared according to Lending and Larkins (1992): mature maize kernels were rifted with a razor at the peripheral region and placed in 2.5% glutaraldehyde. Samples were critically dried and spray coated with gold. Gold-coated samples were then observed with a scanning electron microscope (S3400N; Hitachi).

For transmission electron microscopy (TEM), immature kernels of *dek2* and WT were prepared according to Lending and Larkins (1992), with some modifications: 18 DAP kernels of *dek2* and WT were fixed in paraformaldehyde and postfixed in osmium tetraoxide. After dehydrated in an ethanol gradient, samples were then transferred to a propylene oxide solution and gradually embedded in acrylic resin (London Resin Company). Sections (70 nm) of samples were made with a diamond knife microtome (Reichert Ultracut E). Sample sections were stained with uranyl acetate and poststained with lead citrate. Sample sections were observed with a Hitachi H7600 transmission electron microscope.

Map-based cloning

A population of 3358 homozygous mutant kernels from F_2 ears was used for gene mapping. The chromosome arm location of *dek2* was reported in Neuffer and Sheridan (1980) and this information enabled us to focus on using molecular markers distributed throughout maize (*Zea mays*) chromosome arm 1L for preliminary mapping. Molecular markers for fine mapping (Supplemental Material, Table S2) were

developed to localize the *dek2* locus to a 146-kb region. The corresponding DNA fragments were amplified from *dek2* allele and WT plants using KOD Plus DNA polymerase (Toyobo) and sequenced using a MegaBACE 4500 DNA analysis system (Amersham Biosciences).

Subcellular localization of Dek2

The full-length *Dek2* ORF without the stop codon was cloned into pB7YWG. The recombinant plasmid was extracted with ~1 μg total amount and introduced into tobacco leaf epidermal cells through transient transformation using Bio-Rad PDS-1000/HeTM biolistic particle delivery system. The fluorescence signals were detected using LSM710 (Occult International).

RNA extraction and RT-PCR analysis

Total RNA was extracted with TRIzol reagent (Tiangen) and DNA was removed by a treatment with RNase free DNase I (Takara). Using ReverTra Ace reverse transcriptase (Toyobo) RNA was reverse transcribed to complementary DNA (cDNA). Quantitative real-time PCR (qRT-PCR) was performed with SYBR Green Real-Time PCR Master Mix (Toyobo) using a Mastercycler ep realplex 2 (Eppendorf) according to the standard protocol. Specific primers were designed (Table S2) and the experiments were performed to two independent RNA samples sets. A final volume of 20 ml contained 1 ml reverse transcribed cDNA (1–100 ng), 10 ml 23 SYBR Green PCR buffer, and 1.8 ml 10 mM/liter forward and reverse primers for each sample. Relative quantifiable differences in gene expression were analyzed as described previously (Livak and Schmittgen 2001).

Isolation of mitochondria

For blue native (BN)-PAGE, about 15 g of immature seeds at 18 DAP were harvested and were ground with a mortar and pestle in liquid nitrogen, adding 20 ml of extraction buffer (100 mM tricine, 300 mM sucrose, 10 mM KCl, 1 mM $MgCl_2$, 1 mM EDTA-K, 0.1% BSA, 5 mM DTT, pH 7.4) and 60 μl of plant protease inhibitor cocktail (Sigma-Aldrich, St. Louis, MO). The samples were twice centrifuged at 2600 × *g* for 15 min, after filtration through a Miracloth membrane (Calbiochem, San Diego, CA), the supernatant were then centrifuged at 12,000 × *g* for 25 min to pellet crude mitochondria. The pellet was resuspended in wash buffer (100 mM tricine, 300 mM sucrose, 10 mM KCl, 1 mM $MgCl_2$, 1 mM EDTA-K, 0.1% BSA, pH 7.4) and loaded on sucrose density gradients of 1.5, 2.5, 2.5, 2, and 2 ml containing, respectively, 1.8, 1.45, 1.2, 0.9, and 0.6 M of sucrose diluted in wash buffer. After 90 min of centrifugation at 24,000 rpm at 4°, mitochondria were collected from the 1.2/1.45 M interface and diluted four times in wash buffer. The enriched mitochondria were collected after 20 min of centrifugation at 12,000 rpm at 4°.

BN-PAGE

The enriched mitochondria were resuspended in 50 μl of B25G20 solution (25 mM Bis-Tris, 20% glycerin, pH 7.0), adding 20% n-dodecyl-β-D-maltoside (DDM) to the final concentration of 1% DDM, and gently mixed on ice for 1 hr. After 15 min of centrifugation at 12,000 rpm at 4°, the supernatant was collected and added to the loading buffer before BN-PAGE. The concentration of separation gel was from 4 to 13%. At first electrophoresis was running at 50 V, adding 25 V every 20 min to the final 150 V until the loading dye migrated to the edge of the gel. The gel was stained by Coomassie brilliant blue (Zhang *et al.* 2015).

RNA-sequencing analysis

Total RNA (10 μg) was extracted from endosperm of *dek2* and WT kernels were harvested at 18 DAP, and three *dek2* or WT biological samples were pooled together. The poly-A selected RNA-sequencing (RNA-seq) library was prepared according to Illumina standard instruction (TruSeq Stranded RNA LT Guide). Library DNA was checked for concentration and size distribution in an Agilent2100 bioanalyzer before sequencing with an Illumina HiSequation 2500 system according to the manufacturer's instructions (HiSequation 2500 User Guide). Paired-end reads were aligned to the maize B73 genome build *Zea mays* AGPv2.15 using TopHat 2.0.6 (Langmead *et al.* 2009). Data were normalized as fragments per kilobase of exon per million fragments mapped (FPKM), because the sensitivity of RNA-seq depends on the transcript length. Significant differentially expressed genes (DEGs) were identified as those with a fold change and *P*-value of differential expression above the threshold (fold change >2.0, $P < 0.05$).

Data availability

RNA-seq data are available from the National Center for Biotechnology Information Gene Expression Omnibus (http://www.ncbi.nlm.nih.gov/geo) under the series entry GSE87067.

Results

Kernel development is arrested in dek2

The *dek2-ref* (*dek2-N1315A*) mutant was obtained from the Maize Genetics Cooperation Stock Center. It was crossed to the W22 inbred line to produce an F_2 population that displayed a 1:3 segregation of dek (*dek2/dek2*) and WT (+/+ and *dek2*/+) phenotypes (Figure 1A). Mature homozygous *dek2* kernels were small and flat, along with an empty pericarp at the top (Figure 1B). The 100-kernel weight of *dek2* was only ~32% of WT (Figure 1C).

There was a slight decrease in the amount of total protein (4%), a significant decrease in the amount of zein (21%), and a significant increase in the amount of nonzein (38%) in mature *dek2* endosperm (Figure 2, A–D). Among zein proteins, the 22 kDa α-zein and 19 kDa α-zein proteins were relatively less abundant in *dek2* (Figure 2, A and B). We also found obvious difference in total starch content, and starch granule size was smaller in *dek2* endosperm compared to WT (Figure 2, E and F).

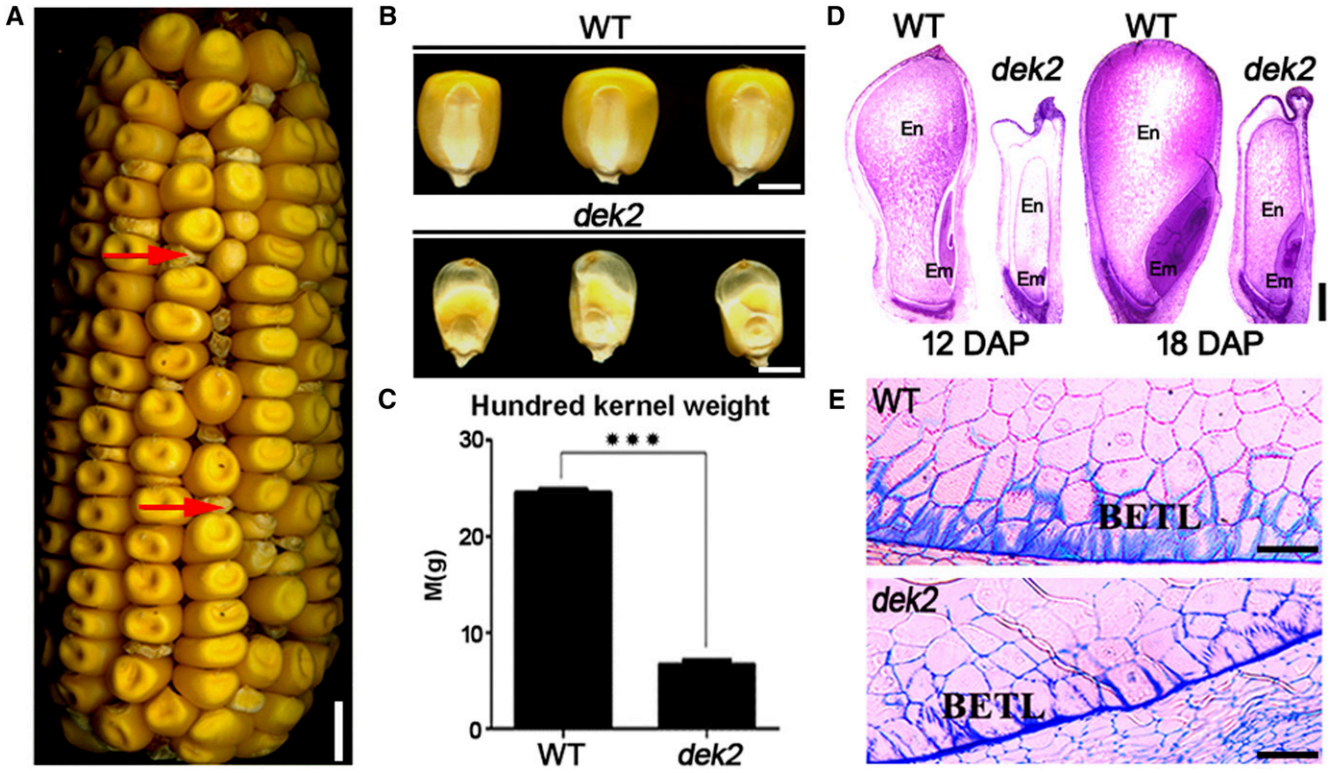

Figure 1 Phenotypic features of maize *dek2* mutant. (A) Mature F_2 ear of *dek2* × W22 population, red arrow identifies the *dek2* kernel. Bar, 10 mm. (B) Randomly selected mature *dek2* and WT kernels from segregated F_2 population. Bar, 5 mm. (C) Comparison of 100-grain weight of randomly selected mature *dek2* and WT kernels in segregated F_2 population. Values are the mean values with SE, $n = 3$ individuals (*** $P < 0.001$, Student's *t*-test). (D) Paraffin sections of 12 DAP and18 DAP *dek2* and WT kernels. Bars, 500 μm. (E) Microstructure of developing endosperm BETL of *dek2* and WT kernels (18 DAP). Bars, 100 μm.

WT and *dek2* kernels of 12 DAP and 18 DAP were analyzed by light microscopy to compare their development. Longitudinal sections of the whole kernel indicated a >6-day developmental delay in *dek2* compared to WT (Figure 1D). Furthermore, paraffin sections of 18 DAP WT and *dek2* endosperm showed the development of basal endosperm transfer layer (BETL) was dramatically arrested in *dek2* kernels (Figure 1E). These results demonstrated that the growth and development of *dek2* kernels are affected.

Positional cloning of Dek2

We performed a map-based approach to clone *Dek2*. After characterizing a population of 438 mutant kernels from the F_2 population, the *dek2* gene was placed between the molecular markers AC191423-10 and AC197739-6, which encompasses a physical region of 486 kb. We further characterized a population of 3358 mutant kernels and placed the *dek2* gene between newly developed molecular markers InDel-1 and SNP-1, which encompasses a physical region of 146 kb. There are eight candidate genes within the interval (gene1: *GRMZM2G100020*, gene2: *GRMZM2G099987*, gene3: *GRMZM5G832651*, gene4: *GRMZM2G123527*, gene5: *GRMZM2G110851*, gene6: *GRMZM2G590033*, gene7: *GRMZM2G479249* and gene8: *GRMZM2G176612*) (Figure 3A). Sequence comparison of the eight candidate genes between WT and mutant alleles revealed a single nucleotide polymorphism (SNP) in gene5 (*GRMZM2G110851*), resulting in an amino acid replacement between the alleles of *dek2-ref* and WT (Figure 3B). There is no sequence difference in other candidate genes. Therefore, *GRMZM2G110851* appeared to be the candidate for the *Dek2*.

Dek2 encodes a P-type PPR protein

The genomic DNA sequence of *GRMZM2G110851* produces a transcript containing a 1893-bp coding sequence and encodes a protein of 630 amino acids (Figure 3B). BLASTP searches of GenBank indicated that *GRMZM2G110851* encodes a P-type PPR protein with 10 PPR repeats (Figure 3B). SNP mutation (G–A) at 914 bp results in an amino acid replacement (Gly–Glu) in the fifth PPR domain in *dek2-ref*.

Two UniformMu insertion lines (UFMu08366, UFMu00444) were identified to carry a *Mu* insertion at 6 bp (*dek2-Mu1*) and 19 bp (*dek2-Mu2*) downstream of the start codon in *GRMZM2G110851*, respectively (Figure 3B). To confirm that *GRMZM2G110851* is the *Dek2* gene, UFMu08366 (*dek2-Mu1*) and UFMu00444 (*dek2-Mu2*) were used for a subsequent allelic test. The allelic test crosses between heterozygous *+/dek2-ref*

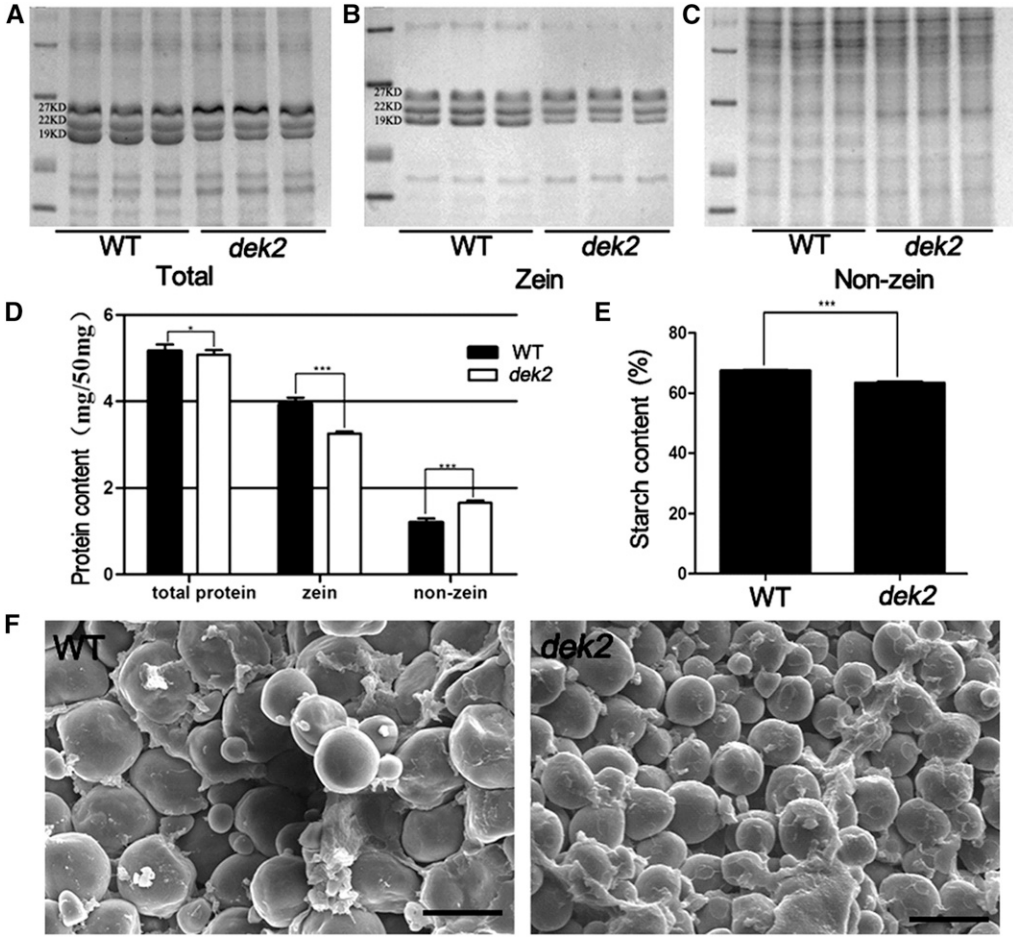

Figure 2 Biochemical analysis and scanning electron microscopy analysis of WT and *dek2* endosperm. (A) SDS-PAGE analysis of total proteins from WT and *dek2* mature endosperm. (B) SDS-PAGE analysis of zein proteins from WT and *dek2* mature endosperm. (C) SDS-PAGE analysis of nonzein proteins from WT and *dek2* mature endosperm. (D) Comparison of total, zein, and nonzein proteins from *dek2* and WT mature endosperm. The measurements were done per milligram of dried endosperm. Values are the mean values with SE, $n = 3$ individuals (* $P < 0.05$, ** $P < 0.01$, *** $P < 0.001$, Student's *t*-test). (E) Comparison of total starch content in WT and *dek2* mature endosperm. The measurements were done per milligram of dried endosperm. Values are the mean values with SE, $n = 3$ individuals (*** $P < 0.001$, Student's *t*-test). (F) Scanning electron microscopy analysis of WT and *dek2* endosperm. Bars, 20 μm.

and +/*dek2-Mu* generated ears exhibiting 3:1 segregation that confirmed that *dek2-Mu1* and *dek2-Mu2* are allelic to *dek2-ref* (Figure 3C). The results demonstrated that *GRMZM2G110851* is the causative gene for *dek2*.

Dek2 is a conserved mitochondria localized protein

The PPR family is prevalently expanded in plants (Fujii and Small 2011). We constructed a phylogenetic tree on the basis of the maize Dek2 full-length protein sequence and homolog protein sequences from other organisms (Figure 4A). The results suggest that Dek2 homologues are highly conserved in angiosperms. And there is no paralog of Dek2 in maize.

PPR proteins are predominantly targeted to plastids or mitochondria (Colcombet *et al.* 2013). To determine the subcellular localization, full-length Dek2 was fused to YFP in a binary vector pB7YWG. The fusion was transiently expressed in tobacco leaf epidermal cells by bombarding, and the fluorescent signal was detected by confocal laser microscopy. The YFP signals were detected in small dots that were identified as mitochondria by red fluorescence of Mito-Tracker pBIN20-MT-RK (Nelson *et al.* 2007; Figure 4B). This result indicated that Dek2 is mitochondrion-targeted protein.

dek2 affects splicing of mitochondrial nad1 intron 1

Previous genetic studies have implicated that a PPR protein may interact with a corresponding mitochondrial or chloroplast RNA (Chen *et al.* 2016; Xiu *et al.* 2016). Because Dek2 is a mitochondrion-targeted P-type PPR protein, we examined the mitochondrial transcripts of 18 DAP *dek2* and WT endosperm. We used specific primers to amplify transcripts with cDNA template for all mitochondrial protein-encoding genes (Table S2). Among 35 genes, only the *nad1* mature transcript was dramatically decreased in *dek2* (Figure 5A).

Then we designed specific primers across adjacent exons of the four introns in *nad1* transcript, respectively (Figure 5B). The result revealed the splicing efficiency of *nad1* intron 1 was decreased in *dek2* compared to WT, while the splicing efficiency of *nad1* intron 2 was not affected and the splicing efficiency of *nad1* intron 3 and intron 4 were even increased. The mature full-length transcript was also reduced (Figure 5B).

P-type PPR proteins were shown to be necessary for splicing of group II introns (Chen *et al.* 2016; Xiu *et al.* 2016). Maize mitochondria have 22 group II introns, including 4 introns of the *nad1* transcript. To investigate the splicing alterations in *dek2* mutants, specific primers were designed for qRT-PCR to

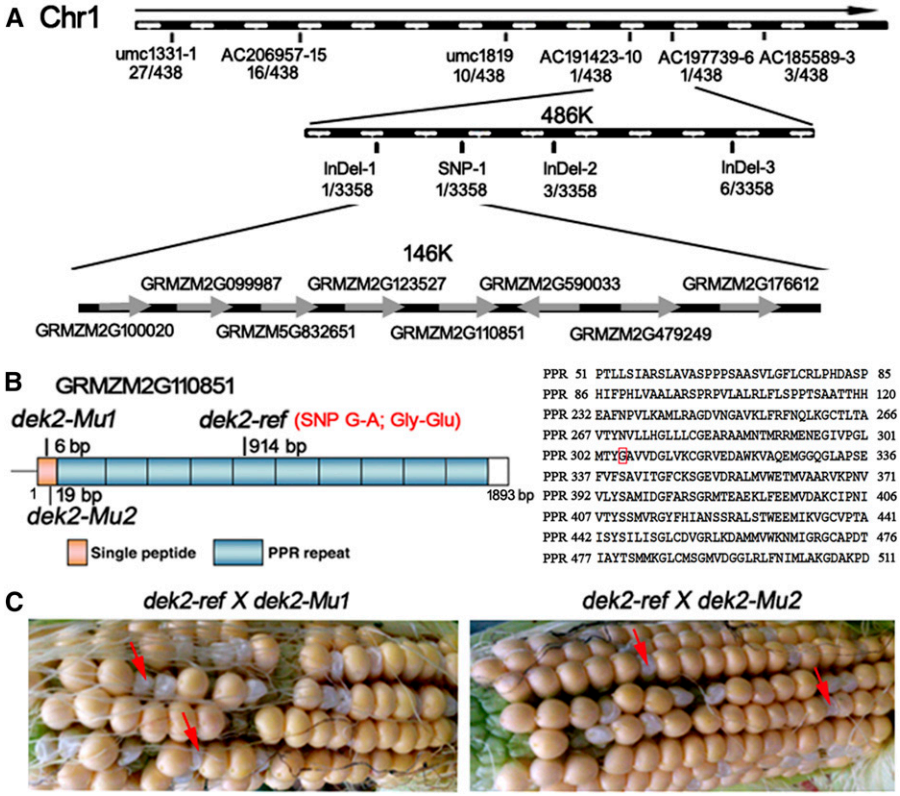

Figure 3 Map-based cloning and identification of *Dek2*. (A) The *Dek2* locus was mapped to a 146-kb region between molecular markers InDel-1 and SNP-1 on chromosome 1, which contained eight candidate genes. See Table S2 online for primer information. (B) Structure and mutation sites of the *Dek2* gene. (C) Heterozygous *dek2-ref* and *dek2-Mu1* and heterozygous *dek2-ref* and *dek2-Mu2* were used in allelism test. Red arrow identifies the mutant kernel.

inspect the 22 mitochondrial group II introns in *dek2* (Table S2). The quantitative differences in spliced exons between *dek2* and WT were compared with amplifying primers across adjacent exons. The results showed the common and single reduction of the *nad1* spliced exon 1–2 fragment in *dek2* (Figure 5C). This result indicated the splicing efficiency of *nad1* intron 1 was decreased in *dek2* and suggested that Dek2 is required for the splicing of mitochondrial *nad1* intron 1 as well as the formation of the *nad1* mature transcript.

dek2 exhibits deficiency of mitochondrial complex I assembly

To further investigate the assembly of respiratory complexes, mitochondrial proteins were isolated from 18 DAP *dek2* and WT endosperm and were analyzed by BN-PAGE. The bands of different complexes were recognized according to Zsigmond *et al.* (2008). The two profiles showed decrease of complex I band and complex I + III^2 super band in *dek2* mutant. And there was a slight increase of complex III band, which might be because of responsible up-regulation to the functional defect of complex I, as previously reported by Xiu *et al.* (2016) (Figure 6A). This result demonstrated that splicing defect in *nad1* intron 1 results in functional reduction of complex I of the respiratory chain.

dek2 exhibits impaired mitochondrial function

We compared the transcript profile of 18 DAP *dek2* and WT endosperm using RNA-seq. Among the 53,520 gene transcripts detected by RNA-seq, significantly DEGs were identified as those with a threshold fold change >2 and *P*-value <0.05. Based on this criterion, 2065 genes showed significant altered expression between *dek2* and the WT. Within the DEGs, 1095 genes could be functionally annotated (annotations were found using BLASTN and BLASTX analyses against the GenBank (http://www.ncbi.nlm.nih.gov/) database). Gene Ontology (GO; http://bioinfo.cau.edu.cn/agriGO/) analysis indicated that DEGs were mostly related to 10 GO terms (Figure 6B and Table S1). Among them, 4 GO terms were closely related to mitochondrial function: GO: 004429 (mitochondrial part, *P*-value = 8.43E-13); GO: 0003942 (GTPase activity, *P*-value = 3.08E-08); GO: 0006119 (oxidative phosphorylation, *P*-value = 0.000853); and GO: 0006626 (protein targeting to mitochondrion, *P*-value = 0.00488).

Fifty-five DEGs were classified to GO: 004429 (mitochondrial part), including *Alternative oxidase 2* (*Aox2*, *GRMZM2G125669*). In plant, alternative oxidases (AOXs) can be activated to maintain the tricarboxylic acid cycle and electron transport when there is an electron transport defect in the cytochrome c pathway (Vanlerberghe and Ordog 2002). The expression of *Aox2* was 1162-fold up-regulated in *dek2* (Table S1). To further validate the expression differences of three *Aox* genes, we performed qRT-PCR and the result showed that both *Aox2* and *Aox3* were dramatically up-regulated (Figure 6C), indicating the alternative respiratory pathway was activated for the inefficient mitochondrial oxidative phosphorylation in *dek2*.

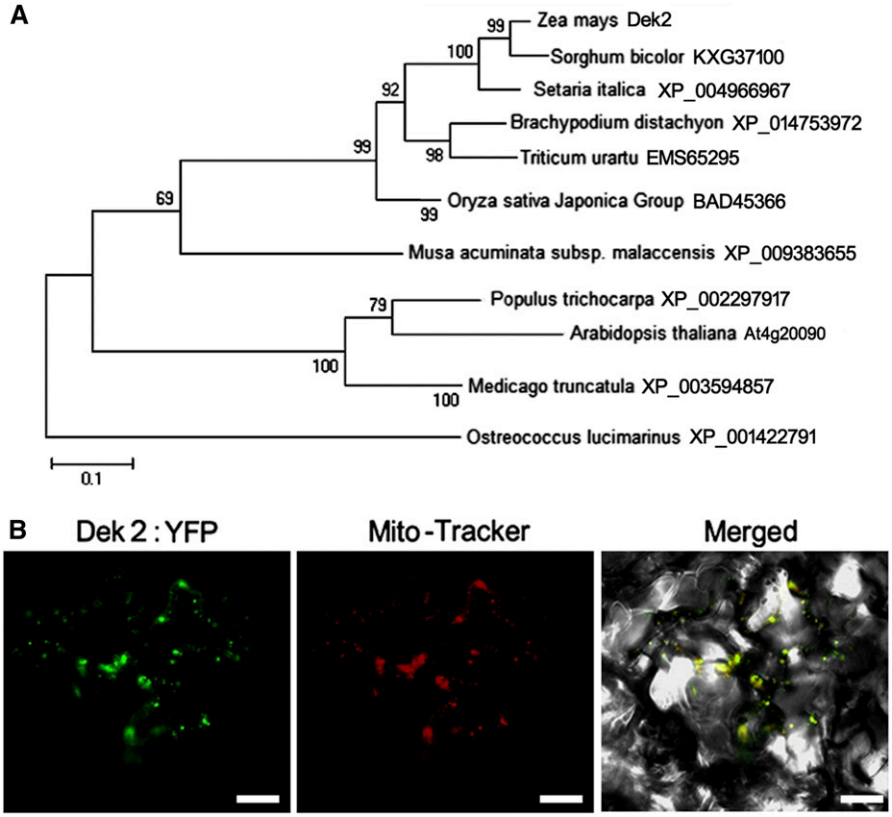

Figure 4 Phylogenetic analysis and subcellular localization of Dek2. (A) Phylogenetic relationships of Dek2 and its homologs. Maize Dek2 and identified homologous proteins in *Sorghum bicolor*, *Setaria italica*, *Brachypodium distachyon*, *Triticum urartu*, *Oryza sativa*, *Musa acuminate*, *Populus trichocarpa*, *Arabidopsis*, *Medicago truncatula*, and *Ostreococcus* were aligned by MUSCLE method in MEGA 5.2 software package. The phylogenetic tree was constructed using MEGA 5.2. The numbers at the nodes represent the percentage of 1000 bootstraps. (B) Subcellular localization of Dek2. The Dek2 fusion protein with YFP at the C terminus (green) and Mito-Tracker pBIN20-MT-RK (red) were transiently expressed in tobacco leaf epidermal cells. Bar, 5 μm.

A mitochondrial function defect in the cytoplasm of 18 DAP *dek2* endosperm was also observed by TEM analysis. Normal activation of the ETC was required for the proper formation of the inner envelope cristaes in mitochondria (Logan 2006). The mitochondria in the WT endosperm formed distinct inner envelope cristaes surrounded with dense matrix, while the internal structure of mitochondria in *dek2* mutant was vague. There was no typical cristaes but only small dots (Figure 6D). The functional reduction of complex I of the respiratory chain causes abnormal morphology of mitochondria in the *dek2* mutant.

Discussion

Dek2 is a newly identified P-type PPR protein required for nad1 intron 1 splicing

Here we define the function of a novel P-type PPR protein, Dek2, that is required for splicing of *nad1* intron 1 in maize mitochondria. To date, at least 46 PPRs involved in pre-RNA editing in the plant mitochondria have been characterized (Hammani and Giege 2014; Li *et al.* 2014; Sun *et al.* 2015). These editing factors mostly belong to the E and DYW subgroups. Fewer splicing-involved PPRs have been studied. The P-type PPR proteins with splicing effect have mainly been studied in *Arabidopsis* mitochondria, including OTP43 (de Longevialle *et al.* 2007), ABO5 (Liu *et al.* 2010), OTP439 and TANG2 (Colas des Francs-Small *et al.* 2014), SLO3 (Hsieh *et al.* 2015), MTL1 (Haili *et al.* 2016), and three nuclear Mat (nMat) genes (Keren *et al.* 2009, 2012; Cohen *et al.* 2014). In maize, much chloroplast transcript splicing involving P-type PPR proteins has been studied. *PPR4* was reported to encode a chloroplast-targeted PPR protein that associated with *trans*-splicing of *rps12* intron 1 (Schmitz-Linneweber *et al.* 2006). PPR5 is another PPR protein that binds to the *trnG*-UCC precursor (Beick *et al.* 2008). THA8 is a short P-type PPR protein associated with splicing of introns in chloroplast *ycf3-2* and *trnA* (Khrouchtchova *et al.* 2012). Recently, a few P-type PPR proteins were found to be involved in maize mitochondrial RNA splicing. EMP16 is specifically required for intron 4 *cis*-splicing of the *nad2* transcript (Xiu *et al.* 2016). Dek35 is the first identified PPR protein responsible for *nad4* transcript splicing (Chen *et al.* 2016).

Both *cis*- and *trans*-splicing of group II introns in the chloroplast and mitochondria require RNA splicing factors. RNA *trans*-splicing probably requires more protein factors than *cis*-splicing, and many more may remain to be identified (de Longevialle *et al.* 2007). The study on OTP43 showed it is specifically required for *trans*-splicing of the first intron in the mitochondrial *nad1* transcript in *Arabidopsis*. Furthermore, nMAT1 and nMAT4 were also reported to be required in splicing of *nad1* intron 1 in *Arabidopsis* (Keren *et al.* 2012; Cohen *et al.* 2014).

dek2-ref is a maize small kernel mutant with a SNP in the fifth PPR domain causing arrested endosperm and embryo

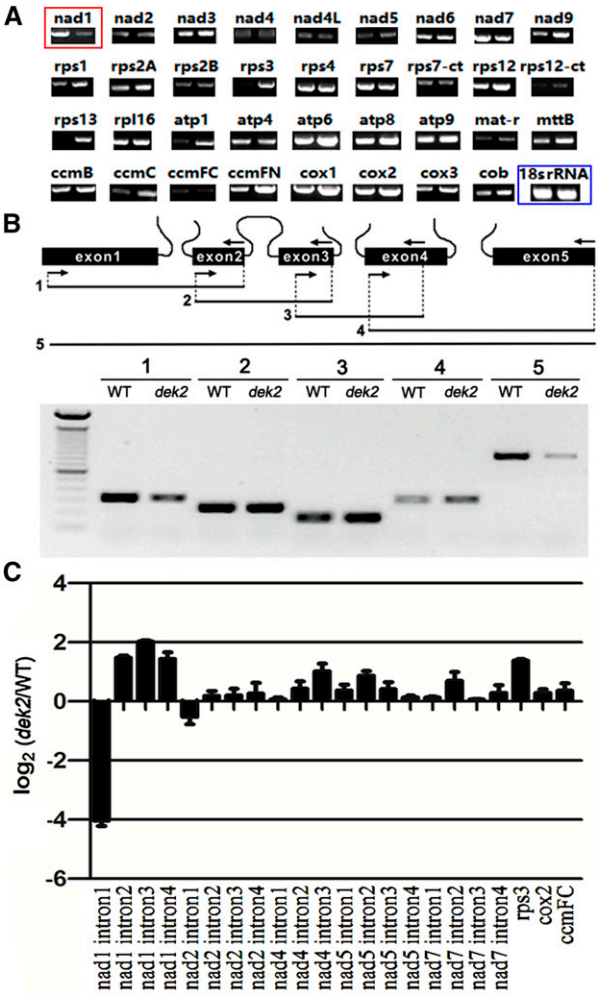

Figure 5 The decrease of *nad1* mature transcript and the splicing deficiency of *nad1* intron 1 in *dek2*. (A) RT-PCR analysis of 35 mitochondria-encoded transcripts in 18 DAP WT (left) and *dek2* (right) endosperm. The RNA was isolated from the same ear segregating for WT and *dek2* mutants.The 18s rRNA served as internal control. Red square identifies *nad1* with decreased transcript abundance; blue square identifies internal control. (B) RT-PCR analysis of *nad1* intron-splicing efficiency in the WT and *dek2* mutant. Structure of the maize mitochondrial *nad1* gene. Intron 1 is a *trans*-spliced intron. The expected amplification products using different primer pairs are indicated. The PCR products were confirmed by sequencing. (C) qRT-PCR analysis of all 22 group II introns in maize mitochondrial genes. Primers spanned adjacent exons, and differences in each spliced fragment were measured. Values are the mean values with SE, n = 3 individuals.

development (Figures 1 and 3). The splicing efficiency of the *nad1* intron 1 was affected in *dek2*, and this alteration of splicing efficiency was not observed in all other mitochondrial group II introns (Figure 5). Phylogenetic analysis showed *Dek2* is not the homologous gene of previously reported *OTP43* (At1g74900), nMAT1 (At1g30010), or nMAT4 (At1g74350), which is required for the *trans*-splicing process of *nad1* intron 1 in *Arabidopsis* (Figure 4). So, Dek2 is a newly identified *nad1* intron 1 *trans*-splicing factor in plant. Further analysis of mitochondrial complexes showed a significant decrease of complex I and supercomplex I + III^2, suggesting a severe defect occurred in complex I assembling as a consequence of a deficient *nad1* transcript (Figure 6). The functional characterization of Dek2 enlarges the understanding of PPR proteins acting in organelle RNA splicing in maize.

Loss of Dek2 resulted in defects in mitochondrial function and kernel development

Most of the characterized PPR mutants affect transcripts encoding proteins of complex I. The defect of complex I assembly always results in severe deficiency in mitochondrial function (Colas des Francs-Small and Small 2014; Hammani and Giege 2014). AOXs can reduce the reactive oxygen species (ROS) levels in situations when ETC complexes are unable to function properly for the maintenance of electron flux. There is rapid activation of AOXs in previously reported PPR mutants (Sun *et al.* 2015; Chen *et al.* 2016; Xiu *et al.* 2016). Respiratory metabolism was blocked in *dek2* as *Aox2*, *Aox3*, and other mitochondrial function-related genes were dramatically up-regulated to rescue the functional tricarboxylic acid cycle (Figure 6 and Table S1). ETC biogenesis was reported to be required for the proper morphology of the cristaes in mitochondria (Logan 2006). In the maize *ppr2263* mutant, the cristaes formed by the inner membrane are strongly reduced and the structurally altered mitochondria were likely less functional than mitochondria with a normal inner structure (Sosso *et al.* 2012). Abnormal morphology of mitochondria was also observed in the *dek2* mutant (Figure 6). The loss of Nad1 (complex I) function results in a defect of ETC biogenesis, which is affecting not only respiratory metabolism but also inner structure of mitochondria.

Dek2 as a nuclear gene-encoded mitochondrial protein is having a profound effect on kernel development when the protein is defective and this has multiple effects, including the delayed formation of BETL and gross retardation of embryo morphogenesis.

BETL develops extensive cell wall ingrowths supporting an enlarged plasma membrane surface that promotes primary nutrient uptake of the endosperm (Pate and Gunning 1972; Thompson *et al.* 2001; Offler *et al.* 2003), which requires high metabolic rates. Therefore, transfer cells are typically rich in mitochondria. The development of BETL was dramatically arrested in *dek2* endosperm (Figure 1). Mutations of the maize *EMP4* gene, *EMP16* gene, and *DEK35* gene encoding PPR proteins also result in a defective transfer cell layer (Gutierrez *et al.* 2007; Chen *et al.* 2016; Xiu *et al.* 2016). The absence of a properly formed transfer cell layer is always correlated with reduced rates of grain filling and seed abortion (Brink and Cooper 1947; Charlton *et al.* 1995). These mutants with arrested BETL development exhibit small and hollow kernels.

The mitochondrial function defect in *dek2* also brings about changes in the expression level of other important energy-consuming biological process-associated genes,

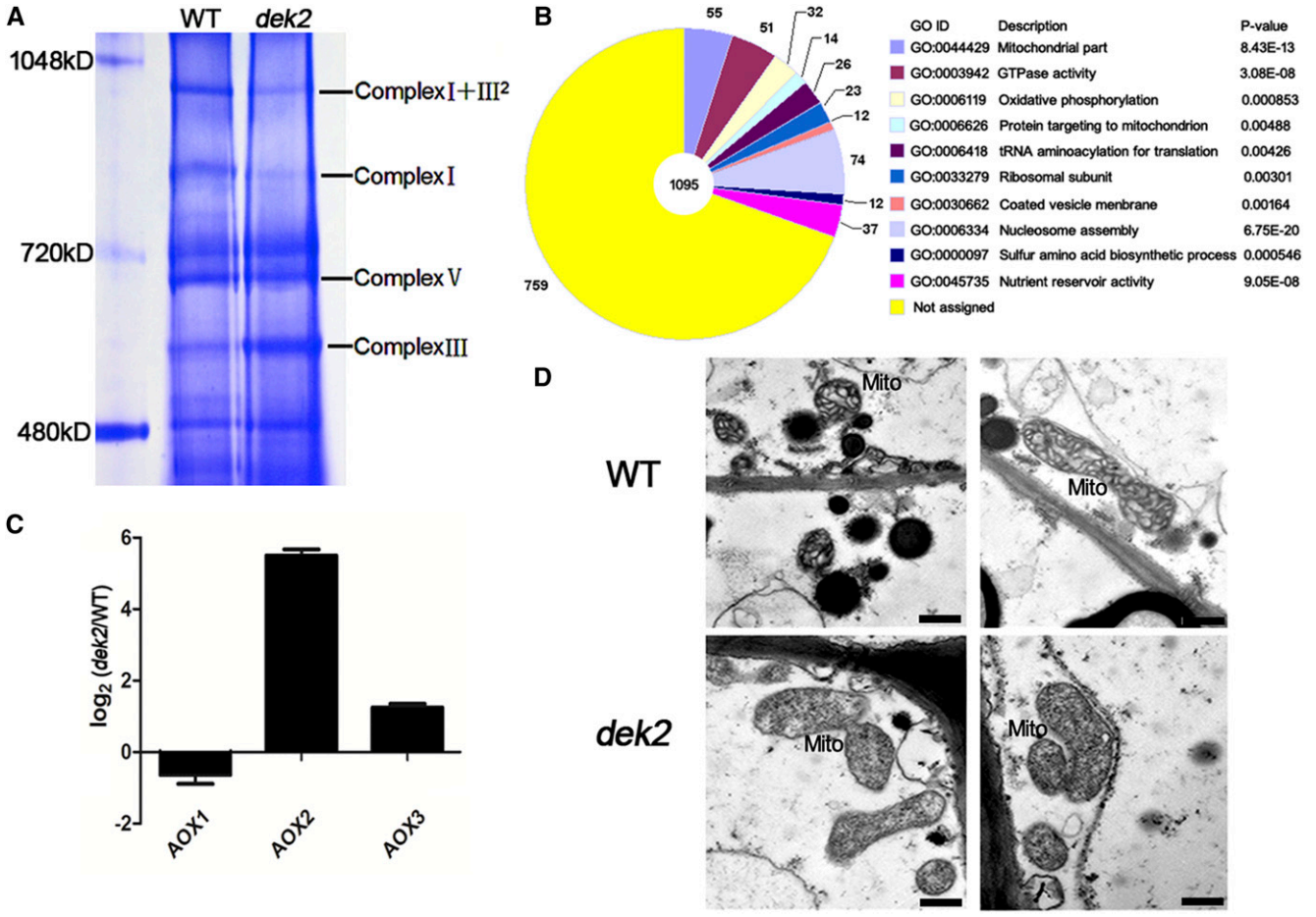

Figure 6 Disrupted mitochondrial function in *dek2* kernels. (A) BN-PAGE analysis of mitochondrial complexes. The positions of supercomplex I + III^2, complex I, complex V, and complex III are indicated. (B) The most significantly related GO terms of the 1095 functional annotated DEGs. The significance and number of genes classified within each GO term are shown. (C) qRT-PCR analysis of genes associated with the alternative respiratory pathway, including *Aox1*, *Aox2*, and *Aox3*. *Actin* served as internal control. Values are the mean values with SE, $n = 3$ individuals. (D) Ultrastructure of developing endosperms of WT and *dek2* (18 DAP) for mitochondria observation. Bars, 1 μm. Mito, mitochondrion.

including sulfur amino acid biosynthetic process, tRNA aminoacylation for protein translation, ribosomal subunit, nutrient reservoir activity, nucleosome assembly, and coated vesicle membrane (Figure 6 and Table S1). The large amount of transcriptionally regulated genes is not the consequence of developmental delay, according to the expression data for developing maize kernels (Chen *et al.* 2014). Sulfur amino acid biosynthetic process (GO:0000097), tRNA aminoacylation for protein translation (GO:0008418), and ribosomal subunit (GO:0033279) are important biological processes for cellular protein accumulation, and genes belong to these classifications were up-regulated might be the responsible regulation to the decreased total protein content in *dek2* (Figure 2). Nutrient reservoir activity in the endosperm, the main storage tissue, largely determines the nutritional value of maize. The most abundant storage protein is zein, which accounts for 50–70% of the total protein, and α-zein is the largest class of zein protein (Holding and Larkins 2006). The genes encoding zein proteins were widely down-regulated in *dek2*, which might be the answer for the dramatically decreased zein protein content (Figure 2). Nucleosome assembly is essential for a variety of biological processes, such as cell cycle progression, development, and senescence (Gal *et al.* 2015), which are also energy-consuming processes. Hence, maize *dek2* mutant affects kernel development, especially BETL formation and embryo morphogenesis, because of mitochondrial function defects and other secondary biological influences.

Acknowledgments

This work was supported by the National Natural Sciences Foundation of China (91335208 and 31425019). There is no conflict of interest.

Author contributions: R.S. and W.Q. designed the experiment. W.Q., Y.Y., X.F., and X.C. performed the experiments. W.Q., Y.Y., and R.S. analyzed the data. W.Q. and R.S. wrote the article.

Literature Cited

Barkan, A., and I. Small, 2014 Pentatricopeptide repeat proteins in plants. Annu. Rev. Plant Biol. 65: 415–442.

Beick, S., C. Schmitz-Linneweber, R. Williams-Carrier, B. Jensen, and A. Barkan, 2008 The pentatricopeptide repeat protein PPR5 stabilizes a specific tRNA precursor in maize chloroplasts. Mol. Cell. Biol. 28: 5337–5347.

Berrisford, J. M., and L. A. Sazanov, 2009 Structural basis for the mechanism of respiratory complex I. J. Biol. Chem. 284: 29773–29783.

Brink, R. A., and D. C. Cooper, 1947 Effect of the *de17* allele on development of the maize caryopsis. Genetics 32: 350–368.

Burger, G., M. W. Gray, and B. F. Lang, 2003 Mitochondrial genomes: anything goes. Trends Genet. 19(12): 709–716.

Chen, J., B. Zeng, M. Zhang, S. Xie, G. Wang *et al.*, 2014 Dynamic transcriptome landscape of maize embryo and endosperm development. Plant Physiol. 166: 252–264.

Chen, X., F. Feng, W. Qi, L. Xu, D. Yao *et al.*, 2016 *Dek35* encodes a PPR protein that affects *cis*-splicing of mitochondrial *nad4* intron 1 and seed development in maize. Mol. Plant. DOI: 10.1016/j.molp.2016.08.008.

Cheng, S., B. Gutmann, X. Zhong, Y. Ye, M. F. Fisher *et al.*, 2016 Redefining the structural motifs that determine RNA binding and RNA editing by pentatricopeptide repeat proteins in land plants. Plant J. 85: 532–547.

Charlton, W. L., C. L. Keen, C. Merriman, P. Lynch, A. J. Greenland *et al.*, 1995 Endosperm development in Zea mays: implication of gametic imprinting and paternal excess in regulation of transfer layer development. Development 121: 3089–3097.

Cohen, S., M. Zmudjak, C. Colas des Francs-Small, S. Malik, F. Shaya *et al.*, 2014 nMAT4, a maturase factor required for nad1 pre-mRNA processing and maturation, is essential for holocomplex I biogenesis in *Arabidopsis* mitochondria. Plant J. 78: 253–268.

Colas des Francs-Small, C., and I. Small, 2014 Surrogate mutants for studying mitochondrially encoded functions. Biochimie 100: 234–242.

Colas des Francs-Small, C., A. Falcon de Longevialle, Y. Li, E. Lowe, S. K. Tanz *et al.*, 2014 The pentatricopeptide repeat proteins TANG2 and ORGANELLE TRANSCRIPT PROCESSING439 are involved in the splicing of the multipartite *nad5* transcript encoding a subunit of mitochondrial complex I. Plant Physiol. 165: 1409–1416.

Colcombet, J., M. Lopez-Obando, L. Heurtevin, C. Bernard, K. Martin *et al.*, 2013 Systematic study of subcellular localization of *Arabidopsis* PPR proteins confirms a massive targeting to organelles. RNA Biol. 10: 1557–1575.

de Longevialle, A. F., E. H. Meyer, C. Andres, N. L. Taylor, C. Lurin *et al.*, 2007 The pentatricopeptide repeat gene *OTP43* is required for *trans*-splicing of the mitochondrial *nad1* intron 1 in *Arabidopsis thaliana*. Plant Cell 19: 3256–3265.

Dudkina, N. V., J. Heinemeyer, S. Sunderhaus, E. J. Boekema, and H. P. Braun, 2006 Respiratory chain supercomplexes in the plant mitochondrial membrane. Trends Plant Sci. 11: 232–240.

Eickbush, T. H., 1999 Mobile introns: retrohoming by complete reverse splicing. Curr. Biol. 9: R11–R14.

Fujii, S., and I. Small, 2011 The evolution of RNA editing and pentatricopeptide repeat genes. New Phytol. 191: 37–47.

Gal, C., K. M. Moore, K. Paszkiewicz, N. A. Kent, and S. K. Whitehall, 2015 The impact of the HIRA histone chaperone upon global nucleosome architecture. Cell Cycle 14: 123–134.

Gutierrez, L., O. VanWuytswinkel, M. Castelain, and C. Bellini, 2007 Combined networks regulating seed maturation. Trends Plant Sci. 12: 294–300.

Haili, N., N. Planchard, N. Arnal, M. Quadrado, N. Vrielynck *et al.*, 2016 The MTL1 pentatricopeptide repeat protein is required for both translation and splicing of the mitochondrial *NADH DEHYDROGENASE SUBUNIT7* mRNA in *Arabidopsis*. Plant Physiol. 170: 354–366.

Hammani, K., and P. Giege, 2014 RNA metabolism in plant mitochondria. Trends Plant Sci. 19: 380–389.

Holding, D. R., and B. A. Larkins, 2006 The development and importance of zein protein bodies in maize endosperm. Maydica 51: 243–254.

Hsieh, W. Y., J. C. Liao, C. Y. Chang, T. Harrison, C. Boucher *et al.*, 2015 The SLOW GROWTH3 pentatricopeptide repeat protein is required for the splicing of mitochondrial *NADH Dehydrogenase Subunit7* intron 2 in *Arabidopsis*. Plant Physiol. 168: 490–501.

Keren, I., A. Bezawork-Geleta, M. Kolton, I. Maayan, E. Belausov *et al.*, 2009 AtnMat2, a nuclearencoded maturase required for splicing of group-II introns in *Arabidopsis* mitochondria. RNA 15: 2299–2311.

Keren, I., L. Tal, C. Colas des Francs-Small, W. L. Araujo, S. Shevtsov *et al.*, 2012 nMAT1, a nuclear-encoded maturase involved in the trans-splicing of nad1 intron 1, is essential for mitochondrial complex I assembly and function. Plant J. 71: 413–426.

Khrouchtchova, A., R. A. Monde, and A. Barkan, 2012 A short PPR protein required for the splicing of specific group II introns in angiosperm chloroplasts. RNA 18: 1197–1209.

Knoop, V., 2013 Plant mitochondrial genome peculiarities evolving in the earliest vascular plant lineages. J. Syst. Evol. 51: 1–12.

Langmead, B., C. Trapnell, M. Pop, and S. L. Salzberg, 2009 Ultrafast and memory-efficient alignment of short DNA sequences to the human genome. Genome Biol. 10: R25.

Lending, C. R., and B. A. Larkins, 1992 Effect of the floury-2 locus on protein body formation during maize endosperm development. Protoplasma 171: 123–133.

Li, X. J., Y. F. Zhang, M. Hou, F. Sun, Y. Shen *et al.*, 2014 Small kernel 1 encodes a pentatricopeptide repeat protein required for mitochondrial nad7 transcript editing and seed development in maize (Zea mays) and rice (Oryza sativa). Plant J. 79: 797–809.

Lid, S. E., D. Gruis, R. Jung, J. A. Lorentzen, E. Ananiev *et al.*, 2002 The defective kernel 1 (dek1) gene required for aleurone cell development in the endosperm of maize grains encodes a membrane protein of the calpain gene superfamily. Proc. Natl. Acad. Sci. USA 99: 5460–5465.

Liu, Y., J. He, Z. Chen, X. Ren, X. Hong *et al.*, 2010 *ABA overly-sensitive 5* (*ABO5*), encoding a pentatricopeptide repeat protein required for *cis*-splicing of mitochondrial *nad2* intron 3, is involved in the abscisic acid response in *Arabidopsis*. Plant J. 63: 749–765.

Liu, Y. J., Z. H. Xiu, R. Meeley, and B. C. Tan, 2013 Empty pericarp5 encodes a pentatricopeptide repeat protein that is required for mitochondrial RNA editing and seed development in maize. Plant Cell 25: 868–883.

Livak, K. J., and T. D. Schmittgen, 2001 Analysis of relative gene expression data using real-time quantitative PCR and the 2(-Delta Delta C (T)) method. Methods 25: 402–408.

Logan, D. C., 2006 The mitochondrial compartment. J. Exp. Bot. 57: 1225–1243.

Lurin, C., C. Andres, S. Aubourg, M. Bellaoui, F. Bitton *et al.*, 2004 Genome-wide analysis of *Arabidopsis* pentatricopeptide repeat proteins reveals their essential role in organdie biogenesis. Plant Cell 16: 2089–2103.

Nelson, B. K., X. Cai, and A. Nebenführ, 2007 A multicolored set of *in vivo* organelle markers for co-localization studies in *Arabidopsis* and other plants. Plant J. 51: 1126–1136.

Neuffer, M. G., and W. F. Sheridan, 1980 Defective kernel mutants of maize. I. Genetic and lethality studies. Genetics 95: 929–944.

Offler, C. E., D. W. McCurdy, J. W. Patrick, and M. J. Talbot, 2003 Transfer cells: cells specialized for a special purpose. Annu. Rev. Plant Biol. 54: 431–454.

Pate, J. S., and B. E. S. Gunning, 1972 Transfer cells. Annu. Rev. Plant Physiol. 23: 173–196.

Qi, W., J. Zhu, Q. Wu, Q. Wang, X. Li *et al.*, 2016 Maize *reas1* mutant stimulates ribosome use efficiency and triggers distinct transcriptional and translational responses. Plant Physiol. 170: 971–988.

Schmitz-Linneweber, C., R. E. Williams-Carrier, P. M. Williams-Voelker, T. S. Kroeger, A. Vichas *et al.*, 2006 A pentatricopeptide repeat protein facilitates the *trans*-splicing of the maize chloroplast *rps12* pre-mRNA. Plant Cell 18: 2650–2663.

Siedow, J. A., and D. A. Day, 2000 Respiration and photorespiration, pp. 676–728 in *Biochemistry and Molecular Biology of Plants*, edited by B. B. Buchanan, W. Gruissem, and R. L. Jones. American Society of Plant Physiologists, Rockville, MD.

Sosso, D., S. Mbelo, V. Vernoud, G. Gendrot, A. Dedieu *et al.*, 2012 PPR2263, a DYW-subgroup pentatricopeptide repeat protein, is required for mitochondrial nad5 and cob transcript editing, mitochondrion biogenesis, and maize growth. Plant Cell 24: 676–691.

Sun, F., X. Wang, G. Bonnard, Y. Shen, Z. Xiu *et al.*, 2015 Empty pericarp7 encodes a mitochondrial E-subgroup pentatricopeptide repeat protein is required for ccmFN editing, mitochondrial function and seed development in maize. Plant J. 84: 283–295.

Thompson, R. D., G. Hueros, H. Becker, and M. Maitz, 2001 Development and functions of seed transfer cells. Plant Sci. 160: 775–783.

Vanlerberghe, G. C., and S. H. Ordog, 2002 Alternative oxidase: integrating carbon metabolism and electron transport in plant respiration, pp. 173–191 in *Advances in Photosynthesis and Respiration*, *Photosynthetic Nitrogen Assimilation and Associated Carbon and Respiratory Metabolism*, Vol. 12, edited by G. H. Foyer, and G. Noctor. Kluwer Academic Publishers, Dordrect, The Netherlands.

Wang, G., X. Sun, G. Wang, F. Wang, Q. Gao *et al.*, 2011 Opaque7 encodes an acyl-activating enzyme-like protein that affects storage protein synthesis in maize endosperm. Genetics 189: 1281–1295.

Wang, G., W. Qi, Q. Wu, D. Yao, J. Zhang *et al.*, 2014 Identification and characterization of maize *floury4* as a novel semidominant opaque mutant that disrupts protein body assembly. Plant Physiol. 165: 582–594.

Xiu, Z., F. Sun, Y. Shen, X. Zhang, R. Jiang *et al.*, 2016 EMPTY PERICARP16 is required for mitochondrial nad2 Intron 4 cis-splicing, complex I assembly and seed development in maize. Plant J. 85(4): 507–519.

Zhang, H. D., Y. L. Cui, C. Huang, Q. Q. Yin, X. M. Qin *et al.*, 2015 PPR protein PDM1/SEL1 is involved in RNA editing and splicing of plastid genes in *Arabidopsis* thaliana. Photosynth. Res. 126: 311–321.

Zsigmond, L., G. Rigó, A. Szarka, G. Székely, K. Otvös *et al.*, 2008 *Arabidopsis* PPR40 connects abiotic stress responses to mitochondrial electron transport. Plant Physiol. 146: 1721–1737.

Communicating editor: J. A. Birchler

Table S1. Gene ontology classifications of DEGs with functional annotation.

GO term	P-value	Gene ID	Description	Fold change	P-value
GO:0006626					
Protein targeting to mitochondrion	4.88E-03	GRMZM2G180971	EF-hand-like domain;Mitochondrial carrier protein	4.45	2.52E-04
		GRMZM2G058432	Mitochondrial inner membrane translocase complex	3.48	1.31E-25
		GRMZM2G174738	Mitochondrial carrier protein	2.07	2.36E-08
		GRMZM2G144101	Mitochondrial inner membrane translocase complex	2.06	6.30E-13
		GRMZM2G002440	GrpE nucleotide exchange factor	2.48	2.43E-04
		GRMZM2G314434	Plant specific mitochondrial import receptor subunit TOM20	2.69	8.95E-11
		GRMZM2G024823	Mitochondrial substrate/solute carrier	3.01	7.53E-05
		GRMZM2G067877	Mitochondrial substrate/solute carrier	2.91	1.26E-11
		GRMZM2G436593	Mitochondrial substrate/solute carrier	2.75	6.45E-04
		GRMZM2G075003	Mitochondrial inner membrane translocase complex	2.05	4.44E-05
		GRMZM2G319878	Mitochondrial inner membrane translocase complex	3.83	3.44E-08
		GRMZM2G030312	GrpE nucleotide exchange factor	4.39	2.32E-19
		GRMZM2G100402	Plant specific mitochondrial import receptor subunit TOM20	3.66	2.30E-11
		GRMZM2G127173	Mitochondrial substrate/solute carrier	4.18	2.47E-04
GO:0006334					
Nucleosome assembly	6.75E-20	GRMZM2G121186	Nucleosome assembly protein (NAP)	3.52	2.15E-17
		AC216889.3_FG008	Histone H2A;Histone-fold	6.89	1.36E-12
		GRMZM2G151826	Histone H2A;Histone core;Histone-fold	5.25	2.22E-19
		GRMZM2G177937	Thioredoxin, conserved site	4.24	3.76E-08
		GRMZM2G079089	Histone H2B;Histone core;Histone-fold	2.38	1.94E-17
		GRMZM2G401308	Histone H1/H5	2.23	5.86E-24
		GRMZM2G448458	Histone H2A;Histone core;Histone-fold	13.87	7.26E-04
		GRMZM2G063896	Histone H4	5.93	1.38E-74
		GRMZM2G479684	Histone H4	5.49	5.54E-171
		GRMZM2G046841	Histone H2B;Histone core;Histone-fold	3.29	1.21E-08
		GRMZM2G056231	Histone H2A;Histone core;Histone-fold	6.10	6.39E-38
		GRMZM2G181153	Histone H4	4.56	8.71E-27
		GRMZM2G349651	Histone H4	7.82	2.27E-34
		GRMZM2G401147	Histone H2B;Histone core;Histone-fold	6.11	2.36E-83
		GRMZM2G008865	Histone H2A;Histone core;Histone-fold	4.60	2.09E-03
		AC191069.3_FG004	IGR protein motif	2.66	1.50E-07
		GRMZM2G163939	Histone H2B;Histone core;Histone-fold	4.31	7.57E-51
		GRMZM2G003306	Histone H2A;Histone core;Histone-fold	6.53	6.29E-109
		GRMZM2G047813	Histone H2A;Histone core;Histone-fold	6.44	2.11E-70
		GRMZM2G054651	TB2/DP1/HVA22 related protein	0.37	2.16E-04
		GRMZM2G069911	Histone H1/H5	3.36	8.68E-14
		GRMZM2G305027	Histone H2B;Histone core;Histone-fold	2.64	2.40E-07
		GRMZM2G140051	Nucleosome assembly protein (NAP)	3.08	9.01E-19

	GRMZM2G112912	Histone H2B;Histone core;Histone-fold	7.14	9.08E-37
	GRMZM2G034157	Heat shock protein Hsp20	7.37	2.07E-102
	GRMZM2G122437	Heavy metal transport/detoxification protein	0.35	2.02E-25
	GRMZM2G145758	Histone core;Histone-fold;Histone H3	4.98	1.29E-14
	GRMZM2G387076	Histone core;Histone-fold;Histone H3	5.91	1.21E-59
	GRMZM2G450937	Leucine-rich repeat;Ribosomal protein L19/L19e	3.18	5.03E-14
	GRMZM2G073275	Histone H4	6.13	6.86E-69
	GRMZM2G118355	Histone core;Histone-fold;Histone H3	2.65	1.22E-46
	GRMZM2G106133	Histone H1/H5	2.19	1.74E-07
	GRMZM2G171387	Histone core;Histone-fold;Histone H3	2.14	2.17E-42
	GRMZM2G084521	Cyclophilin-type peptidyl-prolyl cis-trans isomerase	2.11	2.82E-07
	GRMZM2G305046	Histone H2A;Histone core;Histone-fold	4.30	1.93E-20
	GRMZM2G072855	Histone H4	6.32	2.23E-23
	GRMZM2G472696	Histone H2B;Histone core;Histone-fold	2.36	3.02E-34
	GRMZM2G306258	Histone H2B;Histone core;Histone-fold	5.91	1.09E-39
	GRMZM2G071959	Histone H2B;Histone core;Histone-fold	4.07	5.66E-45
	GRMZM2G332838	Histone H4	5.97	2.47E-108
	GRMZM2G016232	Histone H4	3.15	1.20E-29
	GRMZM2G080274	Histone H1/H5	5.32	3.77E-17
	GRMZM2G042047	Histone H2A;Histone core;Histone-fold	2.63	3.58E-05
	GRMZM2G151726	Histone H2A;Histone core;Histone-fold	2.60	9.70E-15
	GRMZM2G447984	Histone core;Histone-fold;Histone H3	7.24	1.83E-17
	AC212565.3_FG001	Histone H4	4.12	6.53E-68
	GRMZM5G864735	Histone core;Histone-fold;Histone H3	5.53	2.32E-04
	GRMZM2G141432	Histone H2B;Histone core;Histone-fold	2.06	1.66E-09
	GRMZM2G130079	Histone core;Histone-fold;Histone H3	6.34	5.97E-06
	GRMZM2G084195	Histone H4	8.42	5.72E-117
	GRMZM2G057852	Histone H2B;Histone core;Histone-fold	3.74	9.07E-08
	AC196961.2_FG003	Histone H4, conserved site	20.71	9.31E-41
	GRMZM2G421279	Histone H4	6.46	5.42E-105
	GRMZM2G146358	Ribosomal protein L19/L19e conserved site	2.51	1.92E-18
	GRMZM2G144995	NOP5, N-terminal	2.03	8.78E-07
	GRMZM2G176707	Nucleosome assembly protein (NAP)	4.98	3.72E-10
	GRMZM2G109448	Histone H2A;Histone core;Histone-fold	7.05	1.57E-37
	GRMZM2G121221	Histone H1/H5	4.22	3.32E-15
	GRMZM2G164020	Histone H1/H5	4.81	2.15E-49
	GRMZM2G003002	Histone H1/H5	6.96	2.77E-09
	GRMZM2G119071	Histone H2B;Histone core;Histone-fold	7.26	1.36E-12
	GRMZM2G046055	Histone H2A;Histone core;Histone-fold	2.41	2.53E-21
	GRMZM2G107540	Histone H2A;Histone core;Histone-fold	2.31	3.44E-05
	GRMZM2G342515	Histone H2B;Histone core;Histone-fold	8.41	1.80E-69
	GRMZM2G304575	Histone H2B;Histone core;Histone-fold	4.93	1.09E-42
	GRMZM2G078314	Histone core;Histone-fold;Histone H3	7.69	9.37E-65
	GRMZM2G157470	Methyl-CpG DNA binding	2.47	3.87E-03

		GRMZM2G004878	Histone H1/H5	3.69	1.97E-10
		GRMZM2G050833	Histone H2A;Histone core;Histone-fold	2.52	9.77E-11
		GRMZM2G130746	Histone H2A;Histone core;Histone-fold	2.14	3.21E-10
		GRMZM2G149178	Histone H4	4.57	7.26E-55
		GRMZM2G041381	Histone H2A;Histone core;Histone-fold	5.22	2.48E-04
		GRMZM5G883764	Histone H2A;Histone core;Histone-fold	4.62	2.27E-33
		AC233865.1_FG001	Histone H4	3.72	6.47E-47
GO:0044429 Mitochondrial part	8.43E-13	GRMZM2G157018	ATPase,mitochondrial	2.31	7.57E-39
		GRMZM2G144101	Mitochondrial inner membrane translocase complex	2.06	6.30E-13
		GRMZM2G135186	Mitochondrial substrate/solute carrier	2.93	1.43E-24
		GRMZM2G105207	ETC complex I subunit conserved region	2.22	2.95E-05
		AC194341.4_FG002	ATPase,mitochondrial	2.28	2.61E-21
		GRMZM2G010933	Cytochrome c oxidase copper chaperone	31.26	5.63E-17
		GRMZM2G321404	Mitochondrial inner membrane translocase complex	8.85	1.25E-06
		GRMZM2G042078	ATPase,mitochondrial	3.43	5.11E-15
		GRMZM2G152827	Mitochondrial substrate/solute carrier	3.65	5.57E-30
		GRMZM2G064753	Cytochrome c oxidase, subunit Vb	2.52	2.78E-09
		GRMZM2G120876	Porin, eukaryotic type	4.19	1.71E-16
		GRMZM2G171476	Ubiquinol-cytochrome C reductase	2.97	3.45E-24
		GRMZM2G146670	Porin, eukaryotic type	4.09	1.73E-18
		GRMZM2G150616	Porin, eukaryotic type	3.58	8.54E-27
		GRMZM2G038375	Mitochondrial inner membrane translocase complex	2.41	5.73E-09
		GRMZM2G125669	Alternative oxidase	1162.37	6.74E-47
		GRMZM2G058432	Mitochondrial inner membrane translocase complex	3.48	1.31E-25
		GRMZM2G048013	Cytochrome c oxidase, subunit VIIa	2.25	8.50E-12
		GRMZM2G412296	Cytochrome c oxidase, subunit VIIa	4.11	9.06E-15
		GRMZM2G071071	EF-hand-like domain;Mitochondrial Rho-like	5.91	3.29E-39
		GRMZM2G100402	Plant specific mitochondrial import receptor subunit TOM20	3.66	2.30E-11
		GRMZM2G167463	Mitochondrial inner membrane translocase complex	4.47	1.18E-13
		GRMZM2G015401	Mitochondrial substrate/solute carrier	2.95	7.73E-04
		GRMZM2G319878	Mitochondrial inner membrane translocase complex	3.83	3.44E-08
		GRMZM2G103771	Mitochondrial inner membrane translocase complex	0.03	1.05E-14
		GRMZM2G134738	Cytochrome c oxidase, subunit Vb	3.33	4.58E-22
		GRMZM2G069229	ATPase,mitochondrial	8.85	1.13E-07
		GRMZM2G024823	Mitochondrial substrate/solute carrier	3.01	7.53E-05
		GRMZM2G067877	Mitochondrial substrate/solute carrier	2.91	1.26E-11
		GRMZM2G018417	Porin, eukaryotic type	5.27	4.12E-09
		GRMZM2G115049	Porin, eukaryotic type	10.49	7.79E-128
		GRMZM2G064600	Mitochondrial inner membrane translocase complex	6.16	2.92E-11
GO:0003942 GTPase activity	3.08E-08	GRMZM2G134982	Translation elongation factor EFTu/EF1A	3.60	6.19E-04
		GRMZM2G113250	Translation elongation factor EFTu/EF1A	2.87	2.88E-29
		GRMZM2G043822	Beta tubulin, autoregulation binding site	3.70	8.04E-41

GRMZM2G343543	Translation elongation factor EFTu/EF1A	2.85	2.90E-33
AC197246.3_FG001	Ras GTPase;Small GTP-binding protein	3.00	4.27E-05
GRMZM2G157334	Ras GTPase;Ras small GTPase;Ran GTPase	2.54	8.19E-25
AC203173.3_FG004	Translation elongation factor EFTu/EF1A, domain 2	2.22	6.72E-26
GRMZM2G110509	Translation elongation factor EFTu/EF1A, domain 2	2.80	3.16E-26
GRMZM2G037204	Ras GTPase;Small GTP-binding protein	2.52	2.40E-07
GRMZM2G128688	Translation elongation factor EFTu/EF1A, domain 2	4.10	7.83E-07
GRMZM2G071790	Beta tubulin, autoregulation binding site	4.86	2.75E-40
GRMZM2G066191	Beta tubulin, autoregulation binding site	8.28	6.50E-04
GRMZM2G056393	Translation elongation factor EFTu/EF1A, domain 2	3.15	9.64E-05
GRMZM2G122805	Ras GTPase	3.37	1.96E-05
GRMZM2G129155	Dynamin GTPase effector	3.66	5.65E-06
GRMZM2G151193	Translation elongation factor EFTu/EF1A, domain 2	2.50	2.09E-18
GRMZM2G149717	Dynamin central domain;Dynamin	2.70	2.06E-04
GRMZM5G850607	Protein synthesis factor, GTP-binding	2.75	2.34E-16
GRMZM2G117900	Translation elongation factor EFTu/EF1A, domain 2	2.20	5.00E-07
GRMZM2G316232	Protein synthesis factor, GTP-binding	5.31	2.04E-03
GRMZM2G099167	Beta tubulin, autoregulation binding site	3.60	6.97E-11
GRMZM2G098129	Guanylate-binding protein, N-terminal	5.17	3.55E-03
GRMZM2G022269	Translation elongation factor EFTu/EF1A, domain 2	4.08	6.89E-21
GRMZM2G108766	Beta tubulin, autoregulation binding site	3.85	1.74E-03
GRMZM2G107654	Translation elongation factor EFTu/EF1A, domain 2	2.13	1.15E-11
GRMZM2G157462	Dynamin central domain;Dynamin	2.07	3.28E-04
GRMZM2G095851	Translation elongation factor EFTu/EF1A, domain 2	2.31	1.96E-20
AC234515.1_FG003	Beta tubulin, autoregulation binding site	4.02	3.64E-06
GRMZM2G023418	Translation elongation factor EFTu/EF1A, domain 2	2.78	1.01E-04
GRMZM2G313678	Translation elongation factor EFTu/EF1A, domain 2	4.40	7.99E-07
GRMZM2G172932	Beta tubulin, autoregulation binding site	3.56	7.72E-14
GRMZM2G028313	Translation elongation factor EFTu/EF1A, domain 2	2.13	1.72E-07
GRMZM2G149768	Translation elongation factor EFTu/EF1A, domain 2	2.23	2.92E-51
GRMZM2G152466	Tubulin/FtsZ, GTPase domain	4.84	5.65E-176
GRMZM2G005516	Tubulin/FtsZ, GTPase domain	2.55	1.23E-03
GRMZM2G164696	Beta tubulin, autoregulation binding site	3.96	9.52E-17
GRMZM2G354604	Ras GTPase;Ran GTPase;Small GTP-binding protein	3.59	9.29E-196
GRMZM2G153541	Translation elongation factor EFTu/EF1A, domain 2	3.51	9.42E-175
GRMZM2G083243	Beta tubulin, autoregulation binding site	7.81	9.60E-14
GRMZM2G133802	Beta tubulin, autoregulation binding site	2.95	3.64E-07
GRMZM2G011216	Protein synthesis factor, GTP-binding	6.38	9.75E-46
GRMZM2G153292	Tubulin/FtsZ, GTPase domain	5.69	3.34E-210
GRMZM2G154218	Translation elongation factor EFTu/EF1A, domain 2	2.14	1.04E-77
AC233866.1_FG006	Translation elongation factor EFTu/EF1A, domain 2	3.18	5.47E-59
GRMZM2G057535	Translation elongation factor EFTu/EF1A, domain 2	19.51	5.09E-05
GRMZM2G416142	Ras GTPase;Small GTP-binding protein	2.62	1.52E-04
GRMZM2G314647	Dynamin central domain;Dynamin	2.90	5.76E-04

		GRMZM2G156476	Ras GTPase;Small GTP-binding protein	2.72	1.60E-03
		AC209819.3_FG012	Ras GTPase;Small GTPase, Rho type"	2.14	2.67E-03
		GRMZM2G001327	Translation elongation factor EFTu/EF1A, domain 2	2.17	1.85E-27
		GRMZM2G180335	Dynamin central domain;Dynamin	3.72	1.47E-07
GO:0000097 Sulfur amino acid biosynthetic process	5.46E-04	GRMZM2G149751	Cobalamin-independent methionine synthase	3.34	4.50E-09
		GRMZM2G165998	RmlC-like jelly roll fold	4.45	3.12E-25
		GRMZM2G013430	Serine acetyltransferase, N-terminal	6.33	7.05E-04
		GRMZM2G076885	Semialdehyde dehydrogenase, dimerisation domain	2.45	5.58E-06
		GRMZM2G165747	Cobalamin-independent methionine synthase	3.43	2.15E-07
		GRMZM2G165622	Cysteine synthase/cystathionine beta-synthase P-phosphate-binding site	6.76	8.71E-09
		GRMZM2G328893	Cysteine synthase K/M	7.36	3.46E-08
		GRMZM2G036708	Cysteine synthase K/M	3.09	2.21E-07
		GRMZM2G574782	HAD-like domain;Methylthioribulose-1-phosphate dehydratase	2.40	1.93E-05
		GRMZM2G112149	Cobalamin-independent methionine synthase	3.49	2.09E-09
		GRMZM2G005887	Cysteine synthase K/M	2.59	1.90E-32
		GRMZM2G048740	Serine acetyltransferase, N-terminal	2.38	1.86E-03
GO:0006418 tRNA aminoacylation for protein translation	4.28E-03	GRMZM2G148709	Arginyl-tRNA synthetase, class Ic	2.27	5.01E-07
		GRMZM2G083836	Nucleic acid-binding, OB-fold	3.99	5.80E-17
		GRMZM2G701193	Cysteinyl-tRNA synthetase/mycothiol ligase	9.85	9.99E-04
		GRMZM2G101463	Phenylalanyl-tRNA synthetase, class IIc, alpha subunit	2.31	2.10E-08
		GRMZM2G013773	Valyl/Leucyl/Isoleucyl-tRNA synthetase, class Ia, editing	9.76	4.56E-11
		GRMZM2G029027	Arginyl-tRNA synthetase, class Ic	2.46	2.86E-04
		GRMZM2G107089	Anticodon-binding	2.75	2.19E-05
		GRMZM2G094123	Anticodon-binding	2.01	6.09E-09
		GRMZM2G002687	Tryptophanyl-tRNA synthetase, class Ib	2.25	7.02E-06
		GRMZM2G041797	Anticodon-binding	3.49	1.58E-03
		GRMZM5G821551	Anticodon-binding	3.43	6.32E-08
		GRMZM2G071871	Nucleic acid-binding, OB-fold	4.69	1.35E-12
		GRMZM2G012404	RNA-binding S4	6.74	3.58E-03
		GRMZM2G172101	Seryl-tRNA synthetase, class IIa	2.82	1.36E-03
		GRMZM5G817976	Prolyl-tRNA synthetase, class IIa, prokaryotic-type	2.85	3.45E-11
		GRMZM2G057491	Glutathione S-transferase, C-terminal-like	11.76	3.49E-06
		GRMZM2G046932	Glutathione S-transferase, C-terminal-like	2.50	7.04E-09
		GRMZM2G386714	Lysyl-tRNA synthetase, class II, C-terminal	4.39	1.50E-04
		GRMZM2G000481	Rossmann-like alpha/beta/alpha sandwich fold	3.33	1.58E-03
		GRMZM2G082271	Phosphoesterase, DHHA1	2.34	1.18E-05

		GRMZM5G874500	Cysteinyl-tRNA synthetase/mycothiol ligase	2.01	7.10E-06
		GRMZM2G090487	FAD-dependent pyridine nucleotide-disulphide oxidoreductase	346.60	5.11E-03
		GRMZM2G146589	Lysyl-tRNA synthetase, class II, C-terminal	3.56	2.70E-32
		GRMZM2G019121	Nucleic acid-binding, OB-fold	2.95	1.81E-10
		GRMZM2G117870	Valyl/Leucyl/Isoleucyl-tRNA synthetase, class Ia, editing	2.08	3.50E-04
GO:0045735 Nutrient reservoir activity	9.05E-08	GRMZM2G078441	RmlC-like jelly roll fold;Cupin 1	0.23	2.40E-12
		GRMZM2G410134	Bifunctional inhibitor/plant lipid transfer protein/seed storage	0.24	0.00E+00
		GRMZM2G008341	Zein seed storage protein	0.00	5.39E-18
		GRMZM2G045387	Zein seed storage protein	0.00	0.00E+00
		GRMZM2G160739	Zein seed storage protein	0.00	0.00E+00
		GRMZM2G044152	Zein seed storage protein	0.00	9.65E-282
		AF546187.1_FG007	Zein seed storage protein	0.01	0.00E+00
		AF546187.1_FG001	Zein seed storage protein	0.00	0.00E+00
		GRMZM2G088441	Zein seed storage protein	0.00	0.00E+00
		GRMZM2G404688	Bifunctional inhibitor/plant lipid transfer protein/seed storage	0.15	1.47E-14
		GRMZM2G044625	Zein seed storage protein	0.00	0.00E+00
		GRMZM2G088273	Zein seed storage protein	0.00	1.37E-12
		GRMZM2G053120	Zein seed storage protein	0.01	4.02E-15
		AF546188.1_FG005	Zein seed storage protein	0.01	0.00E+00
		AF546188.1_FG007	Zein seed storage protein	0.01	0.00E+00
		AF546188.1_FG001	Zein seed storage protein	0.01	0.00E+00
		AF546188.1_FG003	Zein seed storage protein	0.02	2.25E-48
		GRMZM2G138689	Gliadin/LMW glutenin	0.00	0.00E+00
		GRMZM2G054916	RmlC-like jelly roll fold;Cupin 1	0.03	4.47E-09
		GRMZM2G162992	K Homology, type 1;K Homology	2.08	9.75E-05
		GRMZM2G353268	Zein seed storage protein	0.00	0.00E+00
		GRMZM2G059620	Zein seed storage protein	0.00	0.00E+00
		GRMZM2G026703	RmlC-like jelly roll fold;Cupin 1	0.00	1.14E-08
		GRMZM2G008913	Zein seed storage protein	0.00	4.31E-30
		GRMZM2G060429	Bifunctional inhibitor/plant lipid transfer protein/seed storage	0.07	0.00E+00
		GRMZM2G026939	Zein seed storage protein	0.00	0.00E+00
		GRMZM2G067919	RmlC-like jelly roll fold;Cupin 1	0.18	1.68E-24
		GRMZM2G388461	Zein seed storage protein	0.00	0.00E+00
		AC191050.3_FG003	RmlC-like jelly roll fold;Cupin 1	0.14	2.65E-12
		GRMZM2G166141	RmlC-like jelly roll fold	0.07	9.48E-13
		GRMZM2G346897	Zein seed storage protein	0.00	0.00E+00
		GRMZM2G346895	Zein seed storage protein	0.00	9.84E-282
		GRMZM2G397687	Zein seed storage protein	0.00	0.00E+00
		GRMZM2G088365	Zein seed storage protein	0.00	1.25E-52
		GRMZM2G404459	Zein seed storage protein	0.01	3.59E-03
GO:0033279	3.01E-03	GRMZM2G327564	Ribosomal protein L24, SH3-like	2.31	8.30E-24

Ribosomal subunit					
		GRMZM2G064640	RNA-binding S4	2.39	1.65E-13
		GRMZM2G078985	Ribosomal protein S7	2.69	2.08E-22
		GRMZM5G832108	RNA-binding S4	2.13	4.37E-13
		GRMZM2G090422	Ribosomal protein L13	2.50	9.24E-53
		GRMZM2G163561	Nucleic acid-binding, OB-fold	2.12	2.74E-17
		GRMZM2G070649	Translation protein SH3-like, subgroup	3.03	3.22E-04
		AC233949.1_FG004	ATPase, AAA-type, VAT, N-terminal	6.09	2.26E-19
		GRMZM2G092719	Ribosomal protein S2, conserved site	3.30	3.44E-15
		GRMZM2G058923	Ribosomal protein L18e/L15	2.14	1.85E-03
		GRMZM2G036765	ATPase, AAA-type, VAT, N-terminal	4.83	3.89E-18
		GRMZM2G091921	Ribosomal protein L32p	3.81	1.42E-14
		GRMZM2G122290	Ribosomal protein L1	2.89	5.76E-04
		GRMZM2G168149	Ribosomal protein S5, C-terminal	2.05	1.87E-22
		GRMZM2G703490	ATPase, AAA-type, VAT, N-terminal	5.22	7.18E-04
		GRMZM2G140609	Ribosomal protein S12/S23	2.76	1.06E-07
		GRMZM2G126821	Ribosomal protein S2, conserved site	2.15	1.48E-08
		GRMZM2G092663	Ribosomal protein S5, C-terminal	2.31	9.20E-11
		GRMZM2G110952	Protein of unknown function DUF966	2.43	1.83E-19
		GRMZM2G170336	Ribosomal protein S10, eukaryotic/archaeal	2.68	3.33E-08
		GRMZM2G119169	Ribosomal protein L22/L17	2.48	5.05E-10
		AC210013.4_FG019	Ribosomal protein S5, C-terminal	2.33	1.54E-30
		GRMZM2G163769	Ribosomal protein L22/L17	2.48	1.84E-05
GO:0030662					
Coated vesicle membrane	1.64E-03	GRMZM2G073792	Clathrin, heavy chain, propeller repeat	2.83	8.89E-05
		GRMZM2G143725	Sec23/Sec24 beta-sandwich	2.19	4.60E-03
		GRMZM2G085295	Clathrin, heavy chain, propeller repeat	18.31	1.26E-05
		GRMZM5G874869	Zinc finger, Sec23/Sec24-type	6.89	1.32E-04
		GRMZM2G057576	Clathrin, heavy chain, propeller repeat	2.93	2.25E-06
		GRMZM2G011101	Coatomer, beta subunit	2.76	3.32E-05
		GRMZM5G826171	Sec23/Sec24 beta-sandwich	2.86	9.43E-06
		AC155622.2_FG001	Coatomer, alpha subunit, C-terminal	2.24	2.09E-04
		GRMZM2G378906	Coatomer, beta subunit	3.40	1.64E-06
		GRMZM2G048377	Clathrin, heavy chain, propeller repeat	17.95	7.26E-04
		GRMZM2G075680	Zinc finger, Sec23/Sec24-type	4.42	8.99E-05
		GRMZM2G010054	WD40/YVTN repeat-like-containing domain	2.25	1.56E-03
GO:0006119					
Oxidative phosphorylation	8.53E-04	GRMZM2G157018	ATPase, F0 complex, subunit D, mitochondrial	2.31	7.57E-39
		GRMZM2G070360	ATPase, V1/A1 complex, subunit E	2.02	8.37E-07
		GRMZM2G181151	ATPase, F1/V1/A1 complex, alpha/beta subunit, N-terminal	2.18	8.94E-09
		GRMZM2G101020	ATPase, V0 complex, proteolipid subunit C	3.23	1.45E-12
		AC194341.4_FG002	ATPase, F0 complex, subunit G, mitochondrial	2.28	2.61E-21

	GRMZM2G009638	ATPase, F1 complex, gamma subunit conserved site	2.39	4.64E-17
	GRMZM2G138220	ATPase, F1 complex, delta/epsilon subunit	2.06	1.34E-05
	GRMZM2G042078	ATPase, F0 complex, subunit G, mitochondrial	3.43	5.11E-15
	GRMZM2G079777	ATPase, V1/A1 complex, subunit D	2.42	3.95E-06
	GRMZM2G021331	ATPase, F1/V1/A1 complex, alpha/beta subunit, N-terminal	2.47	4.04E-20
	GRMZM2G113408	ATPase, F1/V1/A1 complex, alpha/beta subunit, N-terminal	3.37	8.35E-60
	GRMZM2G321725	ATPase, F1 complex, gamma subunit conserved site	2.60	8.59E-19
	GRMZM2G144372	ATPase, V1 complex, subunit C	2.67	2.40E-07
	GRMZM2G128995	ATPase, V1 complex, subunit C	2.02	6.60E-04
	GRMZM2G156068	ATPase, F1 complex, OSCP/delta subunit	2.81	1.01E-53
	GRMZM2G069458	ATPase, F1 complex, gamma subunit domain	4.01	3.01E-25
	GRMZM2G041275	ATPase, F1/V1/A1 complex, alpha/beta subunit, N-terminal	3.16	1.65E-14
	GRMZM2G171628	ATPase, F1 complex, delta/epsilon subunit	2.16	1.75E-17
	GRMZM2G177005	ATPase, V0 complex, proteolipid subunit C	2.74	5.38E-15
	GRMZM2G078839	ATPase, V1/A1 complex, subunit E	2.66	4.66E-04
	GRMZM2G069229	ATPase, F0 complex, subunit G, mitochondrial	8.85	1.13E-07
	GRMZM2G421857	ATPase, F1/V1/A1 complex, alpha/beta subunit, N-terminal	2.06	1.69E-14
	GRMZM2G021635	ATPase, V1/A1 complex, subunit D	2.34	1.55E-03
	GRMZM2G028432	ATPase, V0 complex, proteolipid subunit C	2.14	4.87E-07
	GRMZM2G058910	ATPase, V0/A0 complex, 116kDa subunit	2.12	1.54E-03

Table S2. Primers used in this work.

Usage	Primer name	Sequence
Mapping	Umc1331-1s	TTATGAACGTGGTCGTGACTATGG
	Umc1331-1a	ATATCTGTCCCTCTCCCACCATC
	AC206957-15s	TAGCTAGCTCGTGCACTTGG
	AC206957-15a	TAGCTGCGAGAACCTCCTGT
	Umc1819s	TATTCAGCAATGTATTCCCCCTGT
	Umc1819a	GCTGCTCTAAAATCATGCTGATAAAA
	AC191423-10s	TGGCAACGCTTTCGCTTTAC
	AC191423-10a	AGGGGAAATCCCTCAACTGT
	AC197739-6s	ATGGTACAAAACTTCTAGCCAGG
	AC197739-6a	ACGTGTGTGTTTGGTTTCGC
	AC185589-3s	ATTGGCTGAAGGCAGAACCA
	AC185589-3a	GTGGGTCCTCCTCAATATTCACA
	Indel-1s	AGCTTGCAAGGATGCCCATAA

	Indel-1a	AACACCCTGGAGAATCCCTG
	Indel-2s	TGCATTGGCATCAACAGTCG
	Indel-2a	CTAGCTTGCAGTTGAGGGAG
	Indel-3s	CCCCACTAGCTTTGTCTCTGC
	Indel-3a	AGCATCAAATGACGAGGAATGA
	SNP-1s	TTGGTGCGAAAATGGCATGG
	SNP-1a	GCAAGCAGGAGTAGCCATCA
RT-PCR	nad1-F	GGCCCGATCATGAGTGAATA
	nad1-R	GCCCCCTTCAGAAGAAACTT
	nad2-F	GACGGAGGAGAGGAAATGAA
	nad2-R	GCAGTCCACCCTTTCTTTGA
	nad3-F	CTTTCCTATGTCCTTCCCCC
	nad3-R	GAGGAGAGCGAGAGAACGAA
	nad4-F	CAGTCACCCGGAGAAGATTT
	nad4-R	TAATTTGGCGCCTGATTGAC
	nad4L-F	CTGACATTCCATGTTTCCGA
	nad4L-R	GAAGAGAACGAAAGGAGAACAGA
	nad5-F	CGCTCGAACATTGTCTGATT
	nad5-R	GTCCTGGCAAGCTCCTACAG
	nad6-F	TGGAAAAACCAAACCCACAT
	nad6-R	CAAGTTCCCTTGGCGTAGTC
	nad7-F	GTTTTGGCTCGCAATAAAGC
	nad7-R	CAGGTGGGACAAGCTCTAGG
	nad9-F	AGCAAGAAGCGGAACAAAAA
	nad9-R	TATTGATTTGTCCCCTCCCC
	rps1-F	AAGGTGGGCTTCGGATTATT
	rps1-R	TCTTCAGTTTTACGCTTACGCT
	rps2A-F	CAGGAAAGATATTTGCCCCA
	rps2A-R	CCTGTATCTCCGGAAACGAA

	rps2B-F	TCCATGGACCCACGTAAAAT
	rps2B-R	GGCCCCTCTCTGATAAGGAA
	rps3-F	GCAGAAAGGGGCAAAAGTAA
	rps3-R	TCGCGACCCCTACTACATCT
	rps4-F	AGAGTTGGGTTCGATTCCCT
	rps4-R	AGCGACTAGGCCGATCTTTT
	rps7-F	TTCGTTGGAAAAACCTACGC
	rps7-R	ATGAGGAAGGCCGATTTTCT
	rps7-ct-F	TTGAACCTCTTTCACGCTCA
	rps7-ct-R	TTCCGATCGAGATGTATGGA
	rps12-F	CTAGCTGCTTCCATATCGCC
	rps12-R	CGGATCGGGAGTAACCACTA
	rps12-ct-F	TGTACGGTTCTGTAGAGGGACA
	rps12-ct-R	TCCGTTTTCTTTTTATAAGGGC
	rps13-F	TCATGATGATTAAGGGAAGAGTGA
	rps13-R	TTGAATTGAACAGTGTGATTGAT
	rpl16-F	GGTTTTTCCCCACTAACCAA
	rpl16-R	GGGTGCGGAAATAGCTAGAA
	atp1-F	CGTTGCTGGTGAAGAAGCAT
	atp1-R	AAAAGCGGATTTATCCATCG
	atp4-F	AGCCACGTGCTCTAATCCTC
	atp4-R	TCCCTTTCTCTTGGAGCAGA
	atp6-F	CCAAGTCTCTTTTGGGAGCA
	atp6-R	GGCTCCTCGTTTTTATGCAA
	atp8-F	GGCAAGGATCCTCAGTCCTA
	atp8-R	GAGGGTTGGTTTGATTGGAA
	atp9-F	AGGGGCCTCGTCATCTCTAT
	atp9-R	TAGTTGCGAAGGAAAAGCGT
	Mat-r-F	AACGCCTGTTCGCTAAAATC

	Mat-r-R	AGGCTTTGCTCCCCTTTTT
	mttB-F	TTGGTTTAGAATTGCTCGGG
	mttB-R	AGGGGGAACCCTACCGAC
	ccmB-F	AGCCGTCGAAGTGAATGAAT
	ccmB-R	AACGGCTTTTCCATGACTTG
	ccmC-F	ACTTGCAAGGCAAGGAAAAA
	ccmC-R	CCATGGATGCTTTAGCGAGT
	ccmFC-F	GAGAAGCTCAAATCGAACGG
	ccmFC-R	CGCAGCCACTATTTTGACTC
	ccmFN-F	TGAAGATTGTAAGGCGTTTCC
	ccmFN-R	GGATCATCCTGTGGTTACCG
	cox1-F	GGCCCCTCTCTGATAAGGTT
	cox1-R	GTTAAGGCAAAGCCCAAACA
	cox2-F	GTCCTACTTCTGGTGCTGCC
	cox2-R	GAGAATTGCATTTCCGCTTC
	cox3-F	TCAATCCACTTATTCGTTCCC
	cox3-R	GTTTACATACAACCGGGGCA
	cob-F	ATCAAGGCAAGGGGGTAAAT
	cob-R	GGTGTGATCAGTCTCATCCG
	18s rRNA-F	AAACGGCTACCACATCCAAG
	18s rRNA-R	ACTCGAAAGAGCCCGGTATT
RT-PCR and Real-time PCR for splicing efficiency analysis	nad1exon1F	GCAACGTAGAAAGGGTCCTG
	nad1exon2R	TGAGCTGCAGATCGTAATGC
	nad1exon2F	TCGAAATATGCCTTTCTAGGAG
	nad1exon3R	ATTCAGCTTCCGCTTCTGG
	nad1exon3F	GTCATGGCGCAAAAGCAGATATGG
	nad1exon4R	AGAGCAGACCCCATTGAAGA
	nad1exon4F	TCTTCAATGGGGTCTGCTCT
	nad1exon5R	AGGGAGCCATCGAAAGGTGA

	nad2exonF1	GACGGAGGAGAGGAAATGAA
	nad2exonR1	GCCGGGATCATTAAGAGCATAC
	nad2exonF2	CTCGCAGTATGCTCTTAATGATCC
	nad2exonR2	GGAACTGCAGTAATCTTGAATAGGG
	nad2exonF3	TCTACTGGAGCTACCCACTTCGA
	nad2exonR3	GGTTTGCCGTAATGCTGGA
	nad2exonF4	TTCCAGCATTACGGCAAACC
	nad2exonR4	GCAGTCCACCCTTTCTTTGA
	nad4exon1F	GGTCCTATTCTCTGTCCCGTGC
	nad4exon2R	GTAAATCGGTGGTTCCTGTTTGG
	nad4exon2F	TCATTATAGGGGTATGGGGTTCG
	nad4exon3R	CTAGTGCCGGGTAAACTCATATTG
	nad4exon3F	TAGTCCGAACATACCGGGAATTG
	nad4exon4R	CTTACGGATGTATGCATGCAGTC
	nad5exon1F	CGCTCGAACATTGTCTGATT
	nad5exon2R	AGCAGATACTGGAGTGGGAC
	nad5exon2F	GTCACTGCTGGCGTTTTC
	nad5exon3R	TACCTAAACCAATCATCATATC
	nad5exon3F	GATATGATGATTGGTTTAGGTA
	nad5exon4R	GCCAATCGTCGGAATGTG
	nad5exon4F	TTGCCGAATCCGAGTTTG
	nad5exon5R	GTCCTGGCAAGCTCCTACAG
	nad7exon1F	TAATTTGGCGCCTGATTGAC
	nad7exon2R	CTCGATTAATTTCTCAGTCCCTC
	nad7exon2F	GCCTCTTGGCTTATGTCGAG
	nad7exon3R	CCGAACACTTTGTCGCATCT
	nad7exon3F	GAGGGACTGAGAAATTAATCGAG
	nad7exon4R	CTCGACATAAGCCAAGAGGC
	nad7exon4F	AGATGCGACAAAGTGTTCGG

	nad7exon5R	GTTTTGGCTCGCAATAAAGC
	cox2exon1F	GTCCTACTTCTGGTGCTGCC
	cox2exon2R	GAGAATTGCATTTCCGCTTC
	rps3exon1F	GCAGAAAGGGGCAAAAGTAA
	rps3exon1R	CAGAGCGGGACTTCTTTGGTA
	ccmFCexon1F	CGATAGGTCAGCGAAGCGTG
	ccmFCexon1F	AGACCTCGCAAACAACAACGT
	cox2-exonF1	GCTCTGTTATACTCAATGGACGGG
	cox2-exonR1	AGATGAGTTTTGGCTGGTACAACC
	rps3-exonF1	TTTCGGTAAGACTTGATCTGAATCG
	rps3-exonR1	TATCCTTTCCGGGTCTTGATTTGTC
Real-time PCR for expression level analysis	AOX1-F	CCTATTGGACCGTCAAATTACTGC
	AOX1-R	CACTGTTTCCAGCATCATAGCAC
	AOX2-F	CCAAGACGCTGATGGATAAGGT
	AOX2-R	CCACGGTTTCCAGCATCAT
	AOX3-F	CGGCACCGAGAAGCATGA
	AOX3-R	CTGGTCCACTTCCACTCCGT
	actin-AOX-F	ATGGTCAAGGCCGGTTTCG
	actin-AOX-R	TCAGGATGCCTCTCTTGGCC